AAAS
Ultrafast Science
Volume 2021, Article ID 9783514, 22 pages
https://doi.org/10.34133/2021/9783514

Ultrafast Science
A SCIENCE PARTNER JOURNAL

Review Article

Femtosecond Laser Precision Engineering: From Micron, Submicron, to Nanoscale

Zhenyuan Lin and Minghui Hong

Department of Electrical and Computer Engineering, National University of Singapore, 4 Engineering Drive 3, Singapore 117576

Correspondence should be addressed to Minghui Hong; elehmh@nus.edu.sg

Received 17 October 2021; Accepted 10 November 2021; Published 1 December 2021

As a noncontact strategy with flexible tools and high efficiency, laser precision engineering is a significant advanced processing way for high-quality micro-/nanostructure fabrication, especially to achieve novel functional photoelectric structures and devices. For the microscale creation, several femtosecond laser fabrication methods, including multiphoton absorption, laser-induced plasma-assisted ablation, and incubation effect have been developed. Meanwhile, the femtosecond laser can be combined with microlens arrays and interference lithography techniques to achieve the structures in submicron scales. Down to nanoscale feature sizes, advanced processing strategies, such as near-field scanning optical microscope, atomic force microscope, and microsphere, are applied in femtosecond laser processing and the minimum nanostructure creation has been pushed down to ~25 nm due to near-field effect. The most fascinating femtosecond laser precision engineering is the possibility of large-area, high-throughput, and far-field nanofabrication. In combination with special strategies, including dual femtosecond laser beam irradiation, ~15 nm nanostructuring can be achieved directly on silicon surfaces in far field and in ambient air. The challenges and perspectives in the femtosecond laser precision engineering are also discussed.

1. Introduction

Surface engineering in micro-/nanoscales plays a major role in a material's performance improvement [1, 2]. For example, the material's photoelectrical properties can be modified by changing its surface morphology and chemical energy states [3–5]. By tuning its surface chemical composition [6], structure [7, 8], and lattice structure [9], the functions of photoelectrical devices are feasible to be improved. Furthermore, the frictional force [10, 11], adhesivity [12, 13], and wettability [14, 15] behaving on a material interface are also considered to be strongly controlled by the feature sizes and morphologies of the micro-/nanoscale structures. Therefore, multiscale surface engineering is a key issue in developing novel material structures and the analysis of behavior that exist at surfaces and interfaces.

As a noncontact technique working in the atmosphere, laser energy can be confined within a small region, which leads to photothermal or photochemical reactions. Laser direct writing has shown its great ability from micron, submicron, to nanoscale applications, including semiconductor devices [16, 17], micro-/nanofluidics [18–20], biotechnology [21], and sensors [22], on various materials [23–25]. Due to the great three-dimensional (3D) manufacturing ability and extensive material usability, the numerous applications of femtosecond laser precision engineering have been witnessed from academic researches to production lines in the past decades [26–28]. Subdiffraction limited creations at a scale of dozens of nanometers using multiphoton absorption, thresholding, stimulation emission depletion (STED) effect, and incubation effect have been realized in various materials [29–31]. In combining with advanced manufacturing strategies, the feature size of femtosecond laser precision engineering has been reduced to ~15 nm in the lab [32–34], far smaller than the optical diffraction limit, which would be an important and feasible way for the next generation nanofabrication.

Here, we summarize the recent advances of this powerful technology used in micron, submicron, and nanoscale creation. First of all, the development of femtosecond laser processing is introduced, including the emergence, advantages, improvement, and goal of femtosecond laser precision engineering. The interaction between laser and materials under different pulse durations is then discussed, including the

strategies of two-/multiphoton absorption, near-field effect, and incubation effect. Typical strategies using the femtosecond laser precision engineering for micro-/nanomachining are also sketched out. Sections 2, 3, and 4 focus on the recent researches of femtosecond laser precision engineering in micron, submicron, and nanoscale, respectively. For micron-scale processing, femtosecond laser is widely used in transparent material fabrication. The laser-induced plasma-assisted ablation (LIPAA), two-photon absorption (TPA), and direct irradiation are feasible to create 2D/3D microstructures on different transparent materials. In combining with special strategies, such as microlens array (MLA) and laser interference lithography (LIL), the feature size of the femtosecond laser precision engineering can be pushed down to submicron scale. Laser-induced periodic surface structure (LIPSS) is also an available way to achieve periodic structures in submicron. The femtosecond laser-induced nanoscale features can be divided into near-field and far-field creations. In combination with the advanced manufacturing tools, including atomic force microscope (AFM), near-field scanning optical microscope (NSOM), and microsphere, the smallest feature size can be lower than 30 nm, depending on the near-field effect. To pursue the nanofabrication in far field, the strategies of multiphoton absorption (MPA) and incubation effect are developed, the minimum feature size at ~15 nm can be obtained, which may be further reduced by the fine control of the femtosecond laser precision processing. The challenges and perspectives for the femtosecond laser precision engineering are discussed.

2. Basic Theory and Development of Ultrafast Laser Processing

Since the emergence of the first pulse ruby laser and the earliest study of laser processing [35], the unique laser-matter interaction has been widely studied because it can lead to the obvious modification of materials, which is hard to be realized using other means. The material's property affects how the material behaves for a given application. With laser irradiation, the main energy can be injected into the target within a very short time and confined around the focus position. Thus, it is easy to achieve a property modification of the treated surface compared to other areas without laser irradiation. In particular, the laser-induced modification can be well-tuned by changing the laser processing parameters, including laser fluence, pulse number, pulse duration, and polarization, which can achieve properties improvement across multiple length scales, from nanoscale to microscale.

2.1. Interaction between Laser and Materials at Different Pulse Durations. To realize micromanufacturing with high efficiency and precision, it is significant to choose laser lights with suitable wavelength, pulse duration, and beam shape [36]. The laser-matter interaction is required to be detail investigated and studied since it is a dynamic and complex process as many factors should be considered. To achieve desired precision engineering on the specific material substrate, the laser parameters need to be optimized, including laser fluence, repetition rate, pulse duration, processing times, atmosphere, ambient temperature, and processing strategy. The interaction of laser with the material is mainly concluded as the absorption of photon-induced electronic excitation. In many circumstances, the time scale for the electrons with high excitation energy to transform into heat is about one picosecond [36]. During the photothermal process, electrons in the irradiated substrates firstly absorb incident laser energy and soon transfer the absorbed energy to the atoms via intense collisions, which lead to the rise of substrate temperature. While the surface temperature of irradiated substrate increases to the melting or even vaporization points, the substrate will transform from solid to liquid or gas, also the plasma generation. Meanwhile, as the laser pulse is off, the plasma after supercooling can be used for the synthesis of different functional nanomaterials [37]. In details, for metal materials, the main absorption process is free-free transitions. In this case, the kinetic energy of the conduction electrons increases due to the absorption of photon's energy, which results in the temperature rise of the conduction electrons. Through this interaction between electrons and phonons, the absorbed energies are transferred to atoms in the metallic lattice. For the laser interaction with semiconductors, depending on the Drude model, the heating by the free-free transitions leads to an effective conductivity with high frequency, which means not only the high reflectivity but also the shallow penetration depth of incident light. The photon energy of incident light must be larger than the semiconductors' bandgap for strong absorption. In this case, electron-hole pairs can be generated by the absorption of photon energy, corresponding to the interband transition of electrons from the valence band to the conduction band. The laser-induced electron-hole pairs have a considerable kinetic energy $E_g = h\upsilon$, which instantly deliveries to the lattice vibrations and results in the heating of the semiconductor. With high laser fluence irradiation, the high density of generated electrons leads to numerous electron-hole recombination via Auger processes. The optoelectronic properties of semiconductors behave similarly to metals in this case. For the insulating materials, since the energy bandgap $E_g \gg h\upsilon$, such materials are mostly transparent to the incident light. Thus, the interaction between laser and insulating materials should be realized under high laser intensities, which is sufficient to cause multiphoton absorption. In this case, conduction electrons with high concentrations can be generated, which makes the interaction between light and insulating materials become similar to those described for metals and semiconductors.

As one of the key issues for the evaluation of laser precision engineering, the heat-affected zone (HAZ) is affected by the laser parameters and the target materials' properties, including laser fluence, laser pulse duration, absorption coefficient, and thermal conductivity. Mostly, the feature size of HAZ is on a submicron scale, while it can be further reduced via steam- or liquid-assisted laser processing. Under laser irradiation with a pulse duration larger than a few picoseconds, as shown in Figure 1(a), the HAZ would be strong since the electrons is able to transfer the energy to the lattice in nanosecond, which results in the temperature increase of

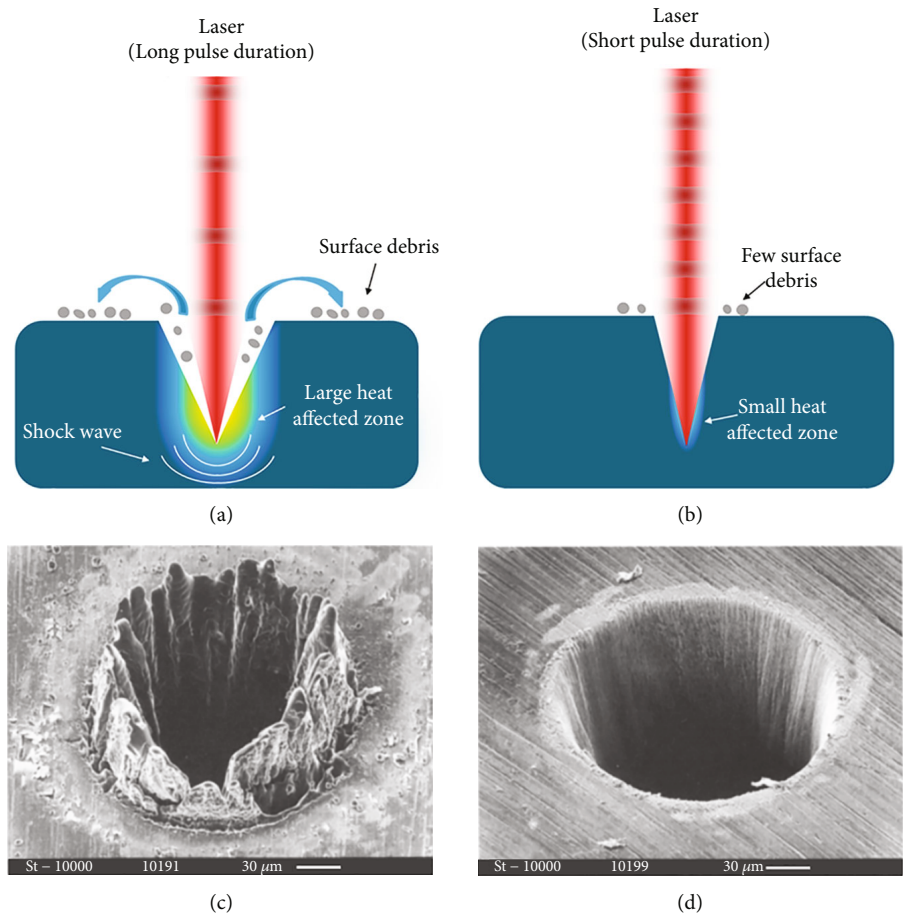

FIGURE 1: Schematic of laser interaction with materials under different pulse durations: (a) long pulse duration and (b) short pulse duration. SEM images of laser ablated holes fabricated on a 100 μm steel foil by (c) 780 nm nanosecond laser of 3.3 ns, 0.5 J/cm^2 and (d) 780 nm femtosecond laser of 200 fs, 0.5 J/cm^2.

samples. The thermal effect also leads to the material expulsion on the sample surface and leaves enormous debris around the irradiated area. For femtosecond pulses, with pulse duration $t_p < 10^{-13}$ s, the absorbed energy cannot be transferred from electrons to the lattice in such a short relaxation time. In this case, the electron-electron interaction can only increase the local electron temperature. For the femtosecond laser interaction with metals, the conduction electrons gas can be heated up to 10^4 K within the femtosecond pulse duration ($<10^{-13}$ s). In a relaxation time of 10^{-13} ~10^{-12} s, the atoms can receive kinetic energy from hot electrons. Thus, atoms are mainly limited in their lattice positions since there is not enough time for energy absorption from electrons within 10^{-14} s. In this case, the HAZ is small, as shown in Figure 1(b). Meanwhile, the irradiated surface is smoother compared to that irradiated by a nanosecond laser. Due to the time of ablation processing being ultrashort, the femtosecond laser ablation can be considered a direct solid-vapor (or solid plasma) transition. In this case, the lattice is heated within several picoseconds, which leads to the creation of vapor and plasma with rapid expansion. Thus, the femtosecond laser-induced surface ablation exhibits low HAZ. Figures 1(c) and 1(d) are the surface ablation under nanosecond and femtosecond laser irradiations, respectively [38]. The molten area surrounding the hole structure drilled on steel foil at a laser fluence of 4.2 J/cm^2 for the laser pulse duration of 3.3 ns can be observed obviously, as shown in Figure 1(c). In this case, there is enough time for the energy to propagate from electrons to lattice and to create a relatively large molten layer. Both vapor and liquid phase steel foils are removed since the vaporization leads to a recoil pressure that expels the liquid. In Figure 1(d), the hole drilled in a 100 μm thick steel foil using a laser fluence of 0.5 J/cm^2 for the laser pulse duration of 200 fs irradiation is shown. The cold process effect of the femtosecond laser fabrication allows the surface precision engineering of metals, which is experimentally demonstrated. As can be seen, there is no existence of the molten area around the irradiated area. Only a few dust distribute around the hole structures. Femtosecond-laser-induced multiphoton absorption is applied to achieve the direct laser writing of solid substrates but the resolution is in the region of 100 to 200 nm. To make nanostructures by laser, photochemical reaction is a feasible approach to bring the feature size to less than 100 nm. This is because the process is based on chemical bond breaking during the laser irradiation of photoresist polymer materials. Followed by a

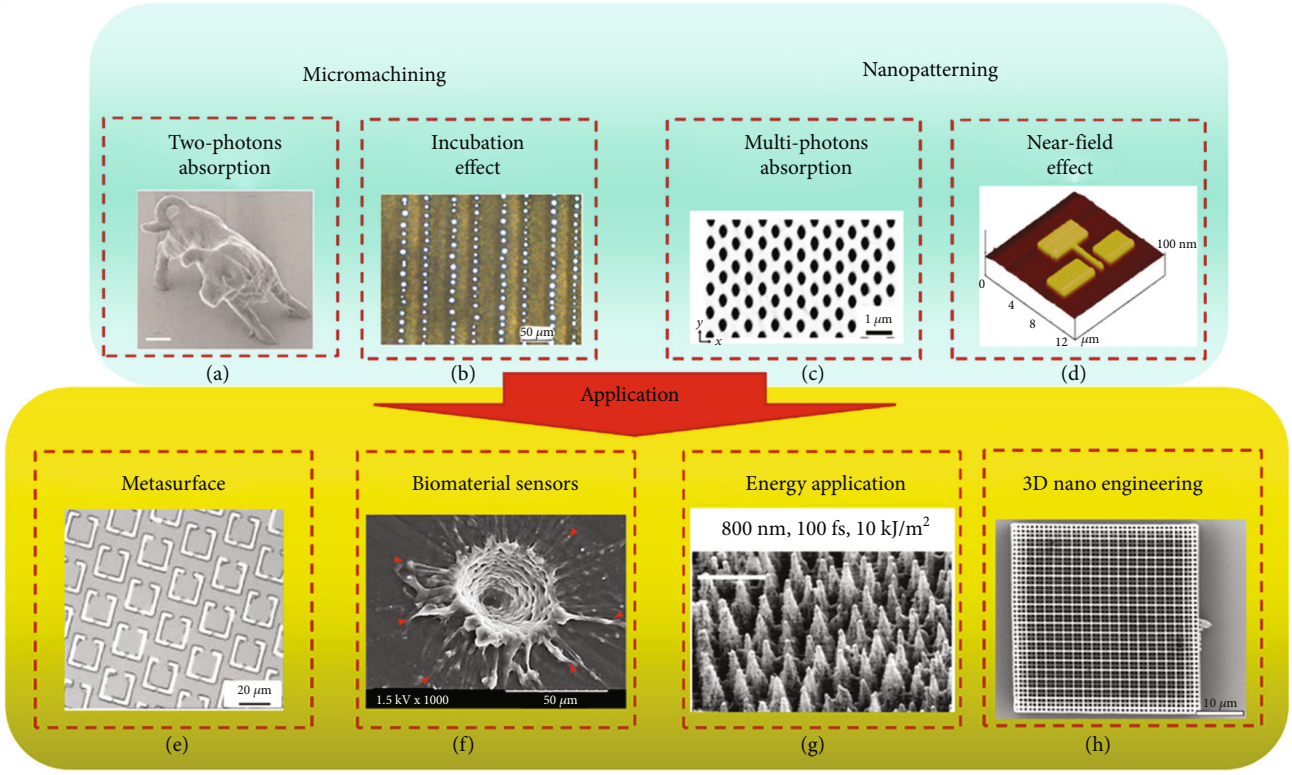

FIGURE 2: Femtosecond laser precision engineering strategies and the related applications: (a) bull sculpture produced by TPA, the scale bar is 2 μm, (b) microhole array fabricated on 150 μm Al film by femtosecond laser direct scanning, (c) wet etching of nanopores fabricated by 3D femtosecond laser writing in YAG crystal, (d) negative metal oxide semiconductor patterns fabricated by femtosecond laser assisting NSOM, (e) functional microstructures made by parallel femtosecond laser processing, (f) surface morphology of HP-PCL achieved by femtosecond laser microperforation, (g) SEM image of laser microstructured Si surface formed in SF_6 with femtosecond laser pulses, and (h) 3D functional photonic crystal fabricated using 1030 nm femtosecond laser in a SZ2080 photoresist without using of photo initiator.

chemical etching, the patterned nanostructures can be transferred from the photoresist down to the solid substrates, which is similar to the photolithography process.

2.2. Strategies for Femtosecond Laser-Matter Interaction. Up to now, many strategies have been proposed for femtosecond laser fabrication in diverse scales, as shown in Figures 2(a)–2(d), including two-/multiphoton absorption, incubation effect, and near-field effect can be employed. Since Kawata et al. reported the 'microbull' sculptures (Figure 2(a)) [39], TPA has been proved as one of the most extensively used means for 3D processing in polymers [40, 41]. Normally, a typical TPA process requires the target material to absorb two photons, with similar or different frequencies, synchronously to achieve sufficient photon energy, which can lead molecules to high energy states. Besides, the sum of photon energies should be high enough for excited molecules to overcome the energy gap between two energy levels [42]. The TPA can only be realized in a high laser intensity, since it is a third-order nonlinear effect. Thus, the femtosecond laser pulses of a 10^{14}~10^{15} W/m^2 peak intensity can localize numerous photons in a tiny focus zone. Under the femtosecond laser irradiation with Gaussian distribution, the TPA-induced threshold effect allows the laser-generated modification to exist at the center of the focal point. In this case, precision engineering with feature sizes of high resolution, even smaller than the diffraction limit can also be created. The femtosecond laser fabrication is mostly processed under the multiple laser pulses irradiation. When using trains of pulses lower than the ablation threshold, the required threshold fluence for the irradiated substrate will be reduced due to the incubation effect [43, 44]. This effect was experimentally observed on several materials, including metals, dielectrics, and semiconductors [45–47]. The incubation effect is attributed to an improvement of laser energy absorption and the increase of the target surface roughness with continuous pulses. As shown in Figure 2(b), Liu et al. reported an interesting experimental phenomenon of self-assembly periodic microhole array creation on Al surface by multiple 800 nm femtosecond laser scanning [48]. The size, shape, and arrangement of such microholes are uniform and tunable, which is different from the hole structures with random distribution in the previous reports. The generation of such periodic microholes is due to the multiple femtosecond laser irradiation-induced incubation effect, which is a feasible way to realize tunable and arbitrary microstructures on the target using single-step manufacturing. Despite the micromachining ability, femtosecond laser is more attractive in nanofabrication since its HAZ is significantly lower than nanosecond and picosecond lasers. As a nonlinear absorption effect, multiphoton absorption is also widely used for nanoscale precision engineering

[49]. For instance, Ródenas et al. proposed that the inner chemical reactivity of YAG crystals could be locally changed in nanoscale, and dense ~110 nm nanopores can be created using femtosecond laser-induced multiphoton absorption [50], as shown in Figure 2(c). In classical optics, the optical diffraction limit has been proved as the reason that leads to the light confinement at feature size larger than the half wavelength of the incident light [51]. At the interface between two different media, an evanescent wave can be excited with laser irradiation [52]. However, with increasing the propagation distance, the intensity of the evanescent wave will perform exponential decay rapidly. Thus, the evanescent wave is strong while it is in the region near the interface of the medium. It means the laser irradiation in near field is a way to break the optical diffraction limit and bring the surface nanomanufacturing down to 100 nm. As shown in Figure 2(c), Lin et al. created negative metal oxide semiconductor patterns employing 400 nm femtosecond laser assisting NSOM nanofabrication strategy [53]. By using this method, 20 ± 5 nm nanoline structures, which are ~1/20 of laser wavelength, can be achieved. Furthermore, NSOM probe with a smaller aperture, which can lead to higher order nonlinear effect, has great potential to use the femtosecond laser-assisted NSOM fabrication to push the resolution lower than 10 nm for the optical device in extreme nanoscale.

In combining with such interesting strategies, femtosecond laser precision engineering is used in various applications. For instance, making a functional metasurface requires fabricating large area, uniform, and even nanoscale surface patterns on sample surfaces. By using MLA femtosecond laser irradiation, it can achieve large area (over 10^5 structures) periodic submicron structures on target surfaces. As shown in Figure 2(e), Hong et al. employed femtosecond laser beam to exposure the MLA and created millions of submicron structures, which can be worked as THz split ring resonator metamaterials [54]. The femtosecond laser is also attractive in the fabrication of biological devices, including biological sensors [55, 56], microfluid [57], and cell surface behavior regulation [58, 59]. Wang et al. fabricated a novel bioresponsive film with dual micro-structured geometries using femtosecond direct perforation of flexible polymer thin film [60], as shown in Figure 2(f). The cold effect of femtosecond laser leads to small HAZ and keeps the irradiated polymer film with less chemical modification, which is beneficial for the growth of biological cells. Besides, the femtosecond laser is also used for flexible smart surface fabrication. Sun et al. proposed a facile creation with the potential wearable application of an ingenious superhydrophobic elastomer skin using femtosecond laser direct writing. Such structures can be used as dynamic and reversible switches between rose petal and lotus leaf modes mimicking human skin surface [61], which demonstrates the great potential and feasibility of femtosecond laser precision engineering in biological devices. As mentioned above, femtosecond laser-matter interaction is different from long laser pulses, while it can excite the bonding electrons of substrate material to a high energy state without energy exchange between electrons and atoms. Especially, the bond-breaking results from the coeffect of multiphoton ionization and photo dissociation, leading to the atoms removal via Coulomb explosion within pulse duration. Therefore, the thermal effect of femtosecond laser ablation is significantly small, even can be completely neglected. It means the laser-induced compositional and structural modifications of the substrate can the minimized. However, with multiple pulse femtosecond laser irradiation, the accumulated heat is still high enough for surface texturing and modification [62]. The formation of highly absorbing nanotextured interfaces via femtosecond laser-induced photochemical reactions is already known to process various materials [63–65]. Figure 2(g) shows the periodic structures generated on the silicon surface in the presence of SF_6 using femtosecond laser irradiation of 800 nm and 10 fs pulse duration [66]; the textured silicon surface exhibits considerable below band gap absorption and photo-induced carrier creation. Femtosecond laser-induced surface chemical modification is used to fabricate a highly crimped surface morphology, which can capture incident light efficiently and perform excellent absorption [67]. In addition to the surface structuring and patterning, another fascinating function of femtosecond precision engineering is the 3D shaping ability. Ever since the report of microbull, micro-/nanoscales 3D manufacturing on various polymers are widely explored. As shown in Figure 2(h), by using 1030 nm femtosecond laser irradiation, high-resolution and good structural quality 3D functional microstructures can be created in the SZ2080 photoresist without employing a twophoton absorbing initiator [68, 69]. Depending on the above descriptions, the femtosecond laser is powerful to realize 2D and 3D structures in micron, submicron, and nanoscale, including surface patterning and internal sculpturing. In the following sections, detail characterization, advantage, limitation, and applications of various strategies for femtosecond laser precision engineering will be discussed.

3. Femtosecond Laser Fabrication in Microscale ($1 \sim 100\ \mu$m)

To form devices with a smooth and clean surface with low damage, it requires fast, stable, selective, and anisotropic fabrication technology. In past decades, femtosecond laser micromachining has been considered a superior material processing tool, capable of generating complex geometries without photomasks and cleanroom facilities, enabling the processing of materials in different atmospheres, as well as in a vacuum. Various targets are feasible to be ablated by the femtosecond laser irradiation [70–72]. Even diamond, with Mons' hardness scale of 10, can be processed [73]. The femtosecond laser-treated hard materials can also be further processed with postchemical etching [74]. In this section, typical strategies, including LIPAA, TPA, and direct ablation are introduced.

3.1. LIPAA. Although laser ablation has been widely used for high-quality and efficient microfabrication of different materials, direct laser irradiation often causes severe damages and cracks during the ablation of transparent materials because of the weak light absorption. To achieve high-quality surface

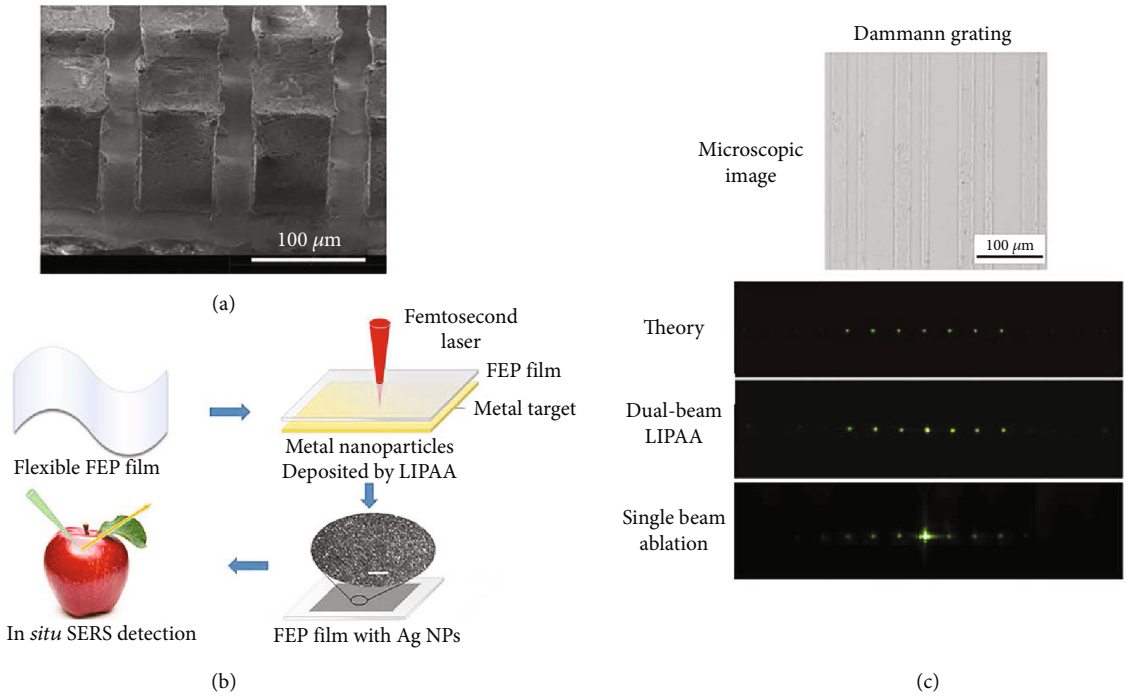

FIGURE 3: Femtosecond laser microprocessing for different applications. (a) Close-up view of microcolumn array fabricated on sapphire, (b) fabrication of flexible surface plasmon resonance film by LIPAA, (c) microscopic images, theoretically designed diffraction patterns, and measured diffraction patterns of femtosecond laser-induced Dammann grating.

ablation, the laser absorption by irradiated substrates should be strong enough. LIPAA is proposed as an available strategy for the surface precision processing of transparent materials [75, 76]. The mechanism of this strategy is that the traditional laser can generate a considerable ablation of transparent substrates via coupling the incident laser with the plasma that came from the metal substrate irradiated by the same light [77, 78]. In this case, the laser microparticle deposition from the metal target creates defects on the back-side of the transparent substrate and leads to the absorption enhancement, which allows the subsequent laser pulses to ablate the transparent substrate easily. Since this method is very simple and performs precise controllability, it has been extensively employed in micromanufacturing, surface patterning, and color marking on transparent substrates [79–81]. The femtosecond LIPAA exhibits more advantages and is able to achieve higher quality and smaller roughness microstructures due to low HAZ. As shown in Figure 3(a), Liu et al. obtained microstructures with high aspect ratio and few cracks on sapphire surfaces by using 800 nm femtosecond LIPAA and following direct laser ablation [82]. By tuning and optimizing the processing parameters, the irradiated sapphire performs a low heating zone and less crack formation. The maximum high aspect ratio of created microgroove arrays on sapphire can be up to 10 : 1 without crack. Meanwhile, the average roughness of the side wall is ~259 nm, which is much smaller than the structure depth (>400 μm). Thus, LIPAA can achieve micron-scale engineering of transparent hard brittle materials with high controllability and precision.

In addition to the cutting of hard brittle transparent material, LIPAA can also be employed in functional device fabrication. Xu et al. reported a one-step and environmentally friendly strategy to create flexible metal coating polymer film for surface enhanced Raman scattering (SERS) detection using femtosecond LIPAA [83], as shown in Figure 3(b). With laser irradiation, Au and Ag particles can be deposited on the fluorinated ethylene propylene film. The Raman signals exhibit great uniformity and the enhancement factor is 5.6×10^7 via R6G Raman probe with respect to bare fluorinated ethylene propylene film. It indicates LIPAA is not only used in the cutting of transparent materials but also able to fabricate functional surfaces. Despite metal materials, it is also feasible to deposit nonmetal particles on substrates using LIPAA [84]. Jiang et al. realized selective graphite films patterning on the glass substrate with a well-control of the LIPAA [85]. The graphite film exhibits strong adhesion resulting from the recast layer of silica and graphite, while the adhesion force and electrical conductivity of the laser-induced metalized pattern can be improved by embedding nickel into the graphite film. Although the LIPAA should deposit metal particles on the substrate surface first, in combination with other methods, it can also realize high surface quality with a lower surface roughness of the transparent materials. As shown in Figure 3(c), inspired by the strategies of double laser beam irradiation and LIPAA, Li et al. proposed a novel dual-beam LIPAA for high-quality sapphire micron-scale processing [86]. In this case, the femtosecond laser is separated into two laser beams with different focusing positions. The

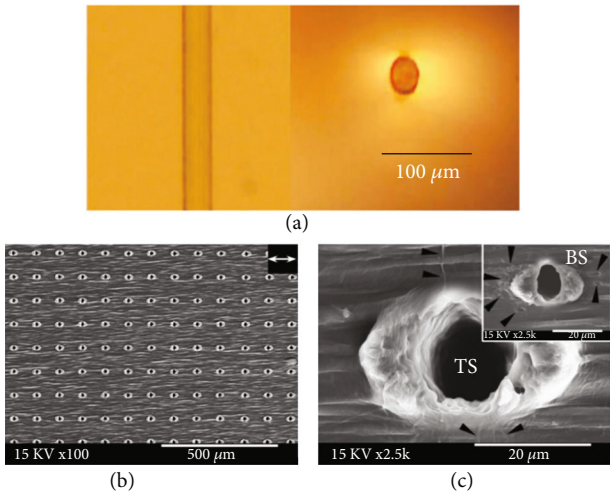

FIGURE 4: (a) Optical microscope images of 30 μm femtosecond laser-induced channel waveguides inside Pr : YLF crystal, (b) dual-microstructured profile of PUX_{HP}-PCL with periodic hole structures, and (c) detail image of single hole structure.

first femtosecond laser is focused on the metal surface for nanoparticle generation, which enables the surface ablation of sapphire by the second laser beam. This method can significantly decrease the ablation threshold of sapphire substrates and the surface roughness of the irradiated surface after the laser ablation. The patterned sapphire can also be used as a Dammann grating and function as an orbital angular momentum generator. The unmodulated power of dual-beam LIPAA fabricated Dammann grating is only 14.3%, which is significantly smaller than the single laser beam-induced substrate (58.5%). Thus, as a hybrid femtosecond laser processing method, LIPAA has great potentials in laser micromachining for functional devices fabrication, especially for the microstructuring of transparent materials. However, the limitation of this method, for instance, the material selectivity, is still required to be improved. Besides, it cannot create nanopatterning using this method since the generation of plasma is hard to be controlled at nanoscale.

3.2. Femtosecond Laser Inscription and Perforation. In addition to the transparent materials, femtosecond laser irradiation can also create microstructures inside crystals. Micron-scale waveguides could confine laser transmission in small regions, which leads to large optical intracavity intensity with respect to the nonwaveguide area. Femtosecond laser irradiation has been regarded as a strong means to create various 3D waveguide structures for different utilizations, exhibiting the advantage of low HAZ, wide feasibility of materials, and ability for mask-free 3D manufacturing [87, 88]. As shown in Figure 4(a), Liu et al. fabricated channel waveguides in a Pr : $LiYF_4$ crystal using 800 nm femtosecond laser [89]. It can be observed that the laser-irradiated area is modified, instead of material removal. The refractive index difference Δn between the modified area and the unirradiated region is confirmed around -9×10^{-4} according to the measurement of the numerical aperture. With a 444.5 nm laser pumping, the crystal with these inscribed waveguides is feasible to generate 605 and 720 nm π-polarized waveguide lasers, which can achieve 66 and 47 mW maximum output powers with efficiencies of 9.5% and 6.3%, respectively. The femtosecond laser is also able to create arbitrary structures inside crystals. Chen et al. successfully achieved S-curved channel waveguides with a low bending loss using femtosecond laser irradiation of hexagonal optical lattice-like waveguide and depressed cladding structures [90]. Such waveguides fabricated in the crystal are used to realize double wavelengths (1064 and 1079 nm) curved waveguide laser with a repetition rate of 31.6 GHz, pulse duration of 16 ps, and maximum signal to noise ratio of 49 dB. The most fascinating advantage of femtosecond laser-induced inscribed crystal is low HAZ and MPA, which leads to less crack and smaller feature size. Furthermore, the femtosecond laser-induced modification of doped ions inside the crystal is also beneficial to fabricate crystal waveguides with novel optoelectrical properties.

The microperforation using femtosecond laser is not only obtained on the hard materials [91, 92] but also realized on the flexible substrates [93, 94]. For instance, as shown in Figures 4(b) and 4(c), Wang et al. created the microperforation on a bioresponsive film to imitate the structure of the endothelial cell basement membrane for vessel development, which can be used for vascular tissue engineering applications [95]. Through tuning the interhole space, the human mesenchymal stem cells developed on the PCL film covered by periodic hole structures and exhibited a high efficiency of cell alignment with few damages. By increasing the growth time, such cells can form regular cell multilayers similar to that exist in the original tunica media. By developing cells of human umbilical vein endothelial on the backside of the PCL film, cells of human umbilical vein endothelial are found to improve the interaction between the mesenchymal stem cells and transmural interdigitation cells through the femtosecond laser-created periodic hole structures, resulting in a quick endothelialization of the laser-treated PCL film surface. The good cultured cell growth is attributed to the low heating effect of femtosecond laser precision engineering, which guarantees no chemical change of irradiated PCL film and high uniformity of created microhole structures. Therefore, in addition to the high precision and be suitable for various materials, femtosecond laser can also provide new surface modification according to the processing requirements.

3.3. Two-Photon Polymerization. It is a key issue to fabricate micron-scale 3D structures using an efficient strategy for the realization of many exciting goals, such as direct 3D printing to make bionic organs and integrated photonic circuits. Two-photon polymerization (TPP) is more attractive than other 3D printing strategies due to its unique approach capable of achieving around 100 nm resolution to fabricate smaller structures. Du et al. developed a flexible hybrid TPP approach that could directly make highly customized microstructures with various desired features. A relatively numerous designed microstructures can be obtained in a time much shorter compared to other lithography methods [96]. As shown in Figure 5(a), including nanolines, 3D Eiffel

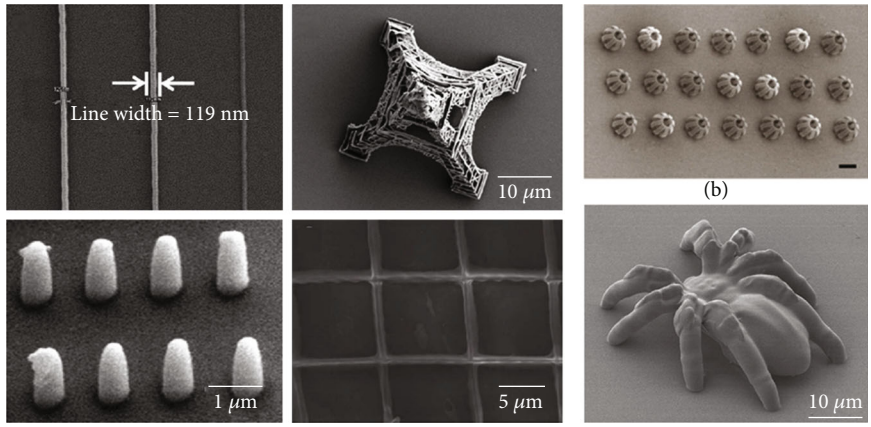

FIGURE 5: 3D precision engineering using TPP effect. (a) SEM images of nanolines, 3D Eiffel Tower, nanopillars, and woodpile structures fabricated by 800 nm femtosecond laser irradiation. (b) SEM image of the microclaw arrays in photopolymers using dual-3D femtosecond laser fabrication, the scale bar is 20 μm. (c) SEM images of the femtosecond laser-created microspider with the blending of bovine serum albumin muscles.

Tower, nanopillars, and woodpile structures can be made by high repetition rate femtosecond laser-induced (800 nm, 80 MHz) TPP technique. Furthermore, gold nanoparticles can also be doped into the photoresist and perform tunable light trapping features. By varying the sizes of the gold nanoparticles, the absorption features can be tuned, which is flexible to meet the requirements of different photonic sensors. These results reveal the potentials of the TPP method to make more functional materials for various applications.

The 3D structuring ability of TPA allows people to realize more bionic structures using femtosecond laser irradiation. Inspired by natural plants, Zhang et al. reported a two-step 3D femtosecond laser manufacturing method for creating intelligent and transformable 3D microactuators using optical polymers [97]. By digital designing, the nanoscale dimensions and distributions of voxels can be achieved, as well as the 3D morphology of the photopolymer can be tailored with good controllability. Figure 5(b) shows that the size of an individual microclaw is ~30 μm, while each micron finger is ~3 μm wide. Such microclaws could be designed to exhibit snatching and reversibly releasing actions, like the muscle of Mollusca. Furthermore, natural musculoskeletal systems are widely considered a feasible and advanced way to fabricate robust and flexible microbots. In combination with programmed artificial musculoskeletal systems and femtosecond laser irradiation, Ma et al. realized 3D microbots in which SU-8 was used as the skeleton and bovine serum albumin, which was a pH-responsive protein, as the intelligent muscle [7]. As shown in Figure 5(c), the microspider is formed after the integration of muscle and polymer, while the microspider has a photoresist body and eight photoresist legs that function as the skeleton. On the junction of each leg, a vacancy is left for muscle integration. In this case, the liveness of BSA is still maintained after femtosecond laser irradiation, which is attributed to the ultrashort pulse duration-induced low thermal diffusion in the biological materials. The successive on-chip TPP strategy that allows programmable integration of multiform materials into complex 3D microfabrication is universal, without limitation to the SU-8 and bovine serum albumin system. Up to now, the TPP strategy still has some limitations. First of all, this method requires the substrates to be transparent at the wavelength of incident laser. Besides, two-photon sensitizers are still the requirement to guarantee the high efficiency processing. However, the above limitations still cannot stop it to become one of the most powerful strategies for femtosecond laser precision engineering due to its high controllability and designability in 3D structuring. In summary, for micron precision engineering, the femtosecond laser is a suitable processing strategy with the capability of high efficiency, high accuracy, low roughness, high reproducibility, and controllability.

4. Femtosecond Laser Submicron Scale Processing (100 nm~1 μm)

The submicron structures are mostly used for functional optoelectronics in the range of near-infrared and mid-infrared wavelengths. Since the scale of submicron structures is mostly in the optical diffraction limit, it is feasible to obtain structures with a feature size of a few hundred nanometers with direct laser irradiation. However, the precision engineering of feature size slightly larger than 100 nm is hard to be realized with the nanosecond or picosecond lasers. In this case, the femtosecond laser is an excellent choice for submicron precision processing due to its nonlinear effect and ability in combining with other advanced tools and strategies [98–100]. In this section, the typical methods for femtosecond laser submicron processing, including MLA, LIPSS, and LIL, will be discussed.

4.1. Femtosecond Laser Fabrication Using MLA. Nanopatterning with a high efficiency, low cost, and high degree of freedom in fabricating nanopatterns is always the objective of nanolithography technologies. To achieve parallel laser fabrication and increase processing efficiency, one of the

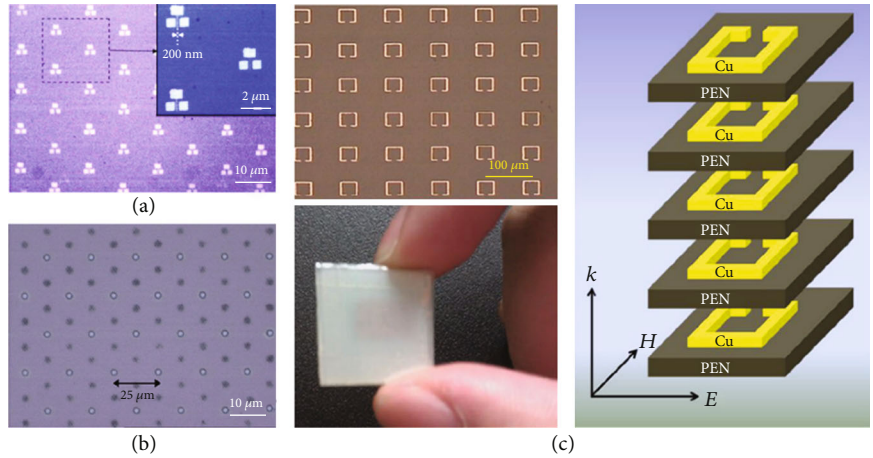

FIGURE 6: Surface patterning via MLA assisting femtosecond laser irradiation. (a) Optical microscope image of field emission transistor structures created on $Ge_1Sb_2Te_4$ film by femtosecond laser irradiation. The inset is a detail image of the structures marked in the dashed square, (b) multifoci patternings on photoresist induced by fractional Talbot effect, and (c) microscopic image and the bonding process of metamaterials for split ring resonators obtained by MLA-assisted 800 nm femtosecond laser manufacturing.

most effective ways is to employ "laser pens" arrays for the realization of numerous patterns synchronously, without using a single laser beam to write the single pattern one by one. MLA is proposed to realize this function for surface submicron patterning with high uniformity and high efficiency [101]. MLA consists of numerous miniaturized lenses which are arranged regularly. The MLA is able to focus incident light into multibeam spot synchronously, which is suitable for various applications, such as optoelectronics, parallel image processing, and optical information transmission. Since it is a noncontact and far-field nanopatterning method that can be processed in parallel, it is hard to achieve feature size smaller than the optical diffraction limit with laser irradiation of longer pulse duration. Thus, the femtosecond laser is used for the creation of precise structures with feature size breaking the optical diffraction limit and manufacture numerous submicron features via MLA synchronously. For instance, Lin et al. used MLA assisting 800 nm femtosecond laser method to create dot arrays, line arrays, and field emission transistor nanostructures on 30 nm $Ge_1Sb_2Te_4$ film surface [102]. Figure 6(a) is the optical microscope image of field emission transistor nanostructures array created by 200 mW laser irradiation at a processing speed of 5 μm/s, and the inset detail image shows that the gate linewidth is ~200 nm. It can be observed that the MLA-assisted femtosecond laser patterning distributes on the target's surface with good uniformity.

The period of surface patterning using MLA-assisted femtosecond laser irradiation is mostly decided by the distribution of each unit on MLA. By using special strategies, more structures with tunable periods can be created on the irradiated surface synchronously. For instance, the fractional Talbot effect of MLA demonstrates that for different distances from the focus plane, and more foci can be found on other planes parallel to the focus plane. As shown in Figure 6(b), using the Talbot effect, Lim et al. realized the patterns with multiple focus points at various fractional Talbot planes [103]. It can be found that, except for the basic foci induced by MLA, additional 'subfoci' distribute around the original foci of the focus plane. The number of multiple focus points is depended on the relative position between the substrate and focus lens, which is the so-called Talbot distance. Such multiple focus points at the partial Talbot plane are available to create high-density patterning using only single-pulse irradiation. Since it is easy to create numerous submicron structures within single-laser pulse irradiation, the MLA can be employed for various functional devices fabrication. As shown in Figure 3(c), Chen et al. fabricated split ring resonators array in large area on flexible polyethylene naphthalate substrates by using MLA lithography [104]. By stacking and combining several layers of femtosecond laser-induced metastructures together, multilayer metasurfaces are obtained. In this case, the resonance effect of multilayer metastructures performs significant enhancement with respect to the single-layer metastructures. Different from other strategies, the working distance of MLA is in the order of incident laser wavelength, which is in the range between the near field and far field. It means both the evanescent wave and propagating wave exist during the MLA-assisted laser fabrication. Thus, it requires high-precision nanostage and smooth substrate surface to create millions of nanostructures with high uniformity synchronously. With the development of information technology nowadays, MLA will be more attractive and applicable widely in manufacturing.

4.2. LIPSS. For the laser-induced damages, LIPSS is a common phenomenon, while this effect has attracted a lot of attention since the short pulse duration laser is easy to generate ripple structures with subwavelength feature size [105, 106]. Sipe et al. demonstrated that the formation of LIPSS under laser irradiation of short pulse duration can be described according to the interaction effect between incident laser and surface scattering lights [107]. It predicts that the laser induced surface wave vectors $\mathbf{k}$, where $|\mathbf{k}| = 2\pi/\Lambda$, should be a function of laser parameters, including the

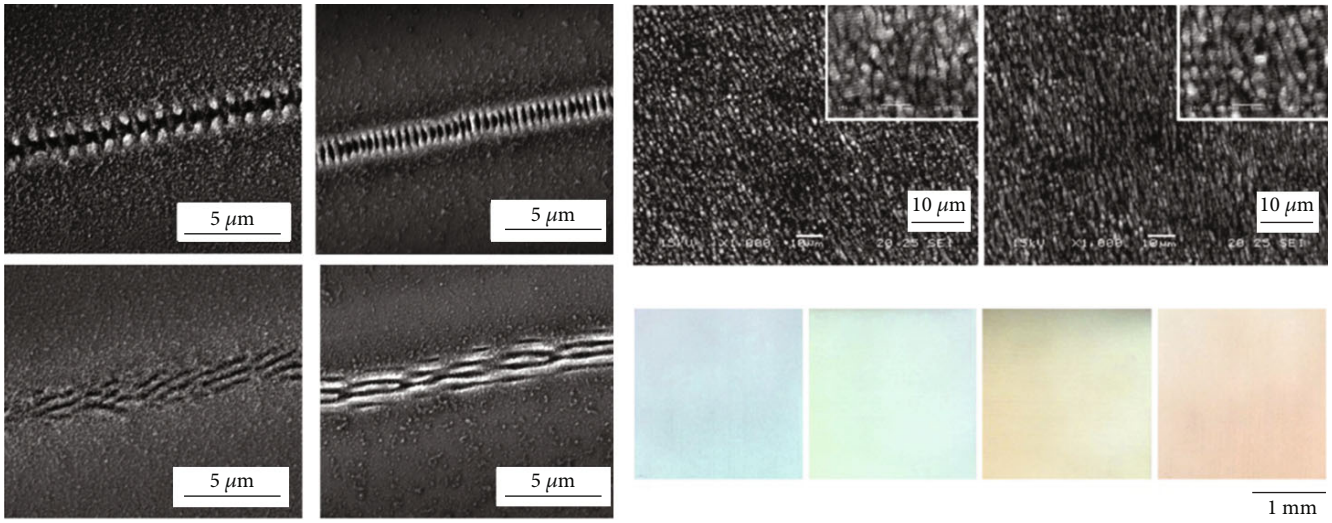

FIGURE 7: (a) LIPSS structures fabricated by 800 nm femtosecond laser at different polarizations. (b) SEM images of morphology evolution of femtosecond laser treated magnesium (Mg) surface with line by line scan and the related photos of coloring effect.

polarization orientation, incident angle θ, and wave vector related to the incident light $\mathbf{k}_L = 2\pi/\lambda$, as well as substrate properties (surface roughness and dielectric constant). Huang et al. further improved the simplified scattering theory of LIPSS formation by taking into account the surface plasmon (SP) [108]. At the very beginning of near subwavelength ripples formation, the interference between the SP and irradiated laser are the main mechanisms. With the development of ripples, the grating induced by the interference will feedback the SP laser coupling, which plays the most significant role for the following structuring. Depending on this theory, the period decreasing performance is attributed to the coeffect of the grating coupling and the optical field distribution. For the direction of LIPSS structures, Bonse et al. proposed that the LIPSS direction is due to the incident light-induced high carrier excitation levels [109]. The LIPSS wave vectors $\mathbf{k}$ can be divided into $\mathbf{k}_x$ and $\mathbf{k}_y$, which are parallel and perpendicular to the polarization of incident light, respectively. In case of high carrier excitation levels, which means under high laser fluence, the wave vector $\mathbf{k}_x$ disappears. Only wave vector $\mathbf{k}_y$ exists and interferes with incident beam $\mathbf{k}_L$. Thus, as shown in Figure 7(a), the directions of LIPSS structures are mostly perpendicular to laser polarization.

The LIPSS with different feature sizes exhibits various physical properties. Guan et al. found that two types of micro-/nanoripples were created on Mg surface with 775 nm femtosecond laser irradiation [110], which performed different colorings, as shown in Figure 7(b). The surface reflectivity measurement reveals that this coloring effect is primarily due to periodic nanostructures being formed and functioned as diffraction gratings, while the surface color intensity is tuned by the morphology of periodic microstructures. SEM images show that the direction of the periodic microstructures is parallel to the incident laser polarization and the corresponding period increases with pulse number. According to the formation mechanism mentioned above, polarization plays an important role in the LIPSS direction [111, 112]. To obtain various surface patterns by using the strategy of LIPSS, Jalil et al. used dual-femtosecond laser beams with orthogonal polarization and time delay to create different LIPSS structures on a bulk Co surface, including triangular, spherical, rhombic, and high spatial frequency structures [113]. The time delay and the laser fluence are the two most important factors influencing the final morphology of LIPSS. The formations of such structures are attributed to the laser-irradiated surface wave interference of orthogonally polarized pulses (spherical structures), self-organization driven by Coulomb repulsion (honeycomb packed triangles structures), and merging between two existing triangular structures (rhombic structures). It indicates the LIPSS formation using multiple laser beams overlapping is complicated and required to be further exploration. Except for the overlapping of two linear polarized laser beams, the circularly polarized laser beam is also feasible to be employed in the double beams overlapping. Fraggelakis et al. demonstrated that homogeneous triangular 2D-LIPSS were obtained using both two linearly crossed polarized beams and double counter-rotating circularly polarized beams [114]. Similarly, rolls, hexagons, and squares structures can be created and tailored by a variation of the interpulse delay. Furthermore, for the LIPSS formation in the case of surface scan processing, the orientation of LIPSS is also influenced by scanning direction and speed, and it would rotate by certain angles. Liu et al. realized the manipulation of the LIPSS orientation on silicon via double femtosecond laser beams irradiation of orthogonal polarization in scanning processing [115]. In this case, the orientation of LIPSS is constantly perpendicular to the scanning direction, regardless of the applied scanning path. Thus, the coupling of multiple laser beams may provide a much more flexible means to control the LIPSS orientation

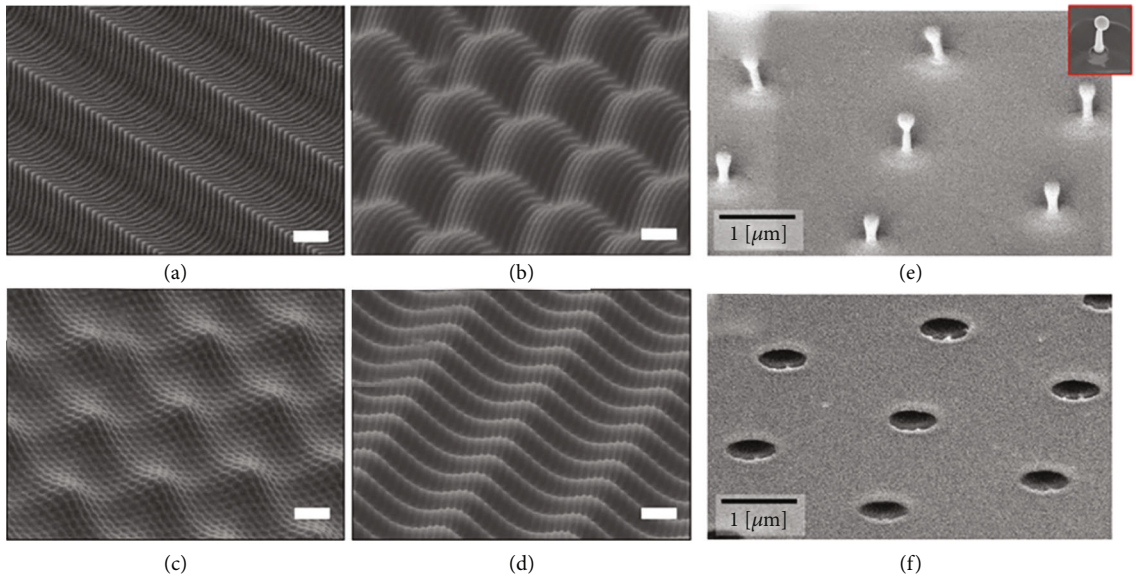

Figure 8: Surface patterning using femtosecond laser interference. (a–d) SEM images of bionic structures, which show various periods, structure morphology, and dimensions. (e) Nanodrop and (f) nanohole structures created by the six-femtosecond laser beam interference; top right inset displays a nanodrop created by the interference of four beams.

without complex rotating devices. In summary, the LIPSS strategy is a feasible way to create large area periodic nanostructures with high efficiency and uniformity. However, the low depth-to-width ratio of the nanostructures using LIPSS constrains its applications in industry, which may be optimized using postchemical etching. Furthermore, this strategy also lacks the ability of free design, which leads it more suitable to be used in the surface coloring, superhydrophobic surface, and grating, rather than the photoelectric devices of complex surface patterning.

4.3. LIL. As a large area, mask-free, and noncontact nanofabrication method, LIL has been studied from 1967 to create numerous periodic structures on and inside targets employing a single step of laser irradiation [116], while the ultrafast laser irradiation is used for the interference manufacturing of metal substrate in 1996 exhibited better processing quality with respect to the nonultrafast laser processing experiments [117]. Since the rapid development of laser beam shaping technology, it is easy to flexibly modulate the optical distribution of femtosecond laser irradiation, which provides new possibilities in LIL processing [118]. The principle of LIL is dependent on the interference of two laser beams, which should be coherent for the formation of horizontal standing wave patterns. The LIL is mostly used for the exposure and record of the patterns on the photoresist. For the interference of two coherent beams, the pattern formed by the standing wave is normally a grating structure. The period $\mathbf{\Lambda}$ is related to light wavelength λ and the angle θ between two incident beams [119]. The common two- laser beam-induced standing wave interference can be calculated as

$$\Lambda = \lambda/(2 \sin \theta). \quad (1)$$

It means that the period of structures fabricated by LIL is normally larger than 100 nm. As the incident angle changes, the nanostructures obtained using LIL are tunable periodic structures, including nanodot, nanonut, and nanorod arrays [120]. Liu et al. fabricated large-area biomimetic hierarchical structures using two 800 nm femtosecond laser beam interference lithography [121]. Due to the excellent capability of surface patterning, different large area periodic structures can be realized and perform great biomimetic ability, such as superhydrophobicity mimicking the lotus. Figures 8(a)–8(d) show the variety of the periodic structures fabricated using four-laser beam interference. The dimension is able to be changed from 1D to 3D, while the revolving angle of the target is tunable up to 90°. The structure height can also be changed by the exposure time, while its range is from 700 to 900 nm for the basic hierarchy and 50 to 100 nm for the secondary one. A series of biomimetic functions can be realized by these periodic hierarchical structures, such as structural coloring and the lotus leaf effect.

The number of laser beams using for the LIL strongly affects the morphology of surface patterning. Thus, three- [122], four- [123], and even six-laser beam [124] LIL processing have been developed. Wang et al. modulated the intensity distribution by using a spatial light modulator (SLM) and realized complicated surface patternings similar to the laser intensity distribution [125]. In combining with three- and four-beam interference, large area nanostructure arrays are obtained with a high output of 1600 μm^2 per pulse. Nakata et al. investigated the surface patterning using six coherent 785 nm femtosecond laser beams for the interference to create nanostructures in a regular hexagonal distribution [126]. The periodic structures are following the numerical simulation depending on the theory of electric fields overlapping. Figures 8(e) and 8(f) show that the

Table 1: Summary of nanoscale precision engineering using femtosecond laser.

Type	Strategy	Wavelength, pulse duration, repetition rate	Feature size	Target	Reference
Near field	ASOM	800 nm, 83 fs, 80 MHz	10 nm	Au	[127]
		1040 nm, 150 fs, 46 MHz	10 nm	Au	[128]
	NSOM	400 nm, 100 fs, 80 MHz	30 nm	Photoresist	[32, 53]
		400 nm, 100 fs, 85 MHz	19.5 nm	Photoresist	[129]
	Microsphere	800 nm, 100 fs, 5 kHz	100 nm	Si	[130]
Far field	MPA	800 nm, 100 fs, 250 kHz	40 nm	SiO_2	[131]
		800 nm, 150 fs, 1 kHz	20 nm	TiO_2	[33]
	STED	800 nm, 200 fs, 76 MHz	40 nm	Resin	[31]
		780 nm, 110 fs, 82 MHz	55 nm	Photoresist	[30]
	LIPSS	800 nm, 50 fs, 1 kHz	32 nm	ZnO	[132]
		400 nm, 38 fs, 80 MHz	40 nm	SU-8	[133]
		800 nm, 50 fs, 100 kHz	20 nm	SiO_2	[134, 135]
	Incubation effect	800 nm, 50 fs, 76 MHz	12 nm	Si	[34]

modular structures achieved on Au thin films are nanodrops and nanohole arrays. The formation of such nanodrop structures can be explained via a solid-liquid phase transition mechanism, where the locally molten gold film is ejected by a coeffect of thermal stress and vapor pressure; then, the melting nanostructure is cooled down. It demonstrates that the LIL using multibeams can provide more designability of the interference patterns for the fabrication of optoelectrical devices. From the surface periodic structuring, LIL can serve as a strategy available to replace traditional methods, for instance, electron beam lithography (EBL) and focused ion beam (FIB) lithography, which are time consuming and costly. Similar to the LIPSS strategy, LIL process also lacks the capability of free design, which can only be slightly improved via multibeam interference. The capability on periodic structuring of this means can be used widely in various applications, including plasmonic, nanophotonic, and other optoelectronic devices fabrication.

5. Femtosecond Laser Nanoscale Processing (10~100 Nm)

Remarkable progress in nanofabrication has been spurred due to the numerous requirements of powerful functional nanostructures and nanodevices. How to improve the feature resolution is a critical issue for next-generation nanoscale precision engineering. Since the required feature size of nanostructures for chip manufacturing become increasingly smaller, it is a big challenge for the traditional lithography to create large area ~10 nm structures at an acceptable cost. Besides, the high device cost and low output limit the large area fabrication by traditional lithography strategies, such as EBL and reactive ion etching (RIE). Thus, novel nanofabrication means with high manufacturing efficiency are important to suffice future industry demands. As shown in Table 1, the advanced approaches using the femtosecond laser processing in near field, such as ASOM, NSOM lithography, and microsphere, can achieve 10~100 nm fabrication resolution that breaking the optical diffraction limit. However, the evanescent waves can only work near the substrate surface, which limits its ability of large area nanofabrication. Thus, the femtosecond laser-induced creation of ~100 nm structures in far field is attractive and worth studying. Strategies based on MPA, STED, LIPSS, and incubation effect can fabricate structures with sub-50 nm feature size on different materials including polymers (Resin, Photoresist, and SU-8), dielectric materials (SiO_2 and TiO_2), and semiconductor materials (Si and ZnO). These technologies, which can be used in far field and in ambient air, possess great potentials and can be widely applied in future nanoscale precision engineering.

5.1. Near-Field Femtosecond Laser Processing. Since the evanescent wave decreases quickly with the propagation distance in near field, it works only in a tiny area near the medium's interface, which can be employed to fabricate nanostructures much smaller than the wavelength. Chimmalgi et al. proposed a controllable surface nanomachine that can be realized by femtosecond laser irradiation using a sharp probe tip to generate the local field enhancement in the near field [127]. As shown in Figure 9(a), nanopatternings of sub-15 nm on the thin Au layers were achieved. The numerical predictions of the spatial optical field distribution of intensity below the silicon AFM tip indicated that the high resolution is attributed to local electric field enhancement. It provides an attractive method for extreme nanofabrication due to its ~10 nm spatial resolution and high efficiency achievable via the simultaneous irradiation of multitip arrays. Near-field scanning optical lithography is superior to the other direct writing strategies, such as RIE and EBL, because it can process in ambient air and be easily controlled at a reasonable cost [129]. Figures 9(b) and 9(c) show 20 ± 5 nm nanodot and nanoline arrays [32], which exhibit a one-twentieth wavelength resolution and half of NSOM probe aperture diameter, respectively. In combining with an NSOM and a 400 nm femtosecond laser of 100 fs pulse duration, Lin et al. achieved nanostructures breaking the optical resolution and further reduced it to sub-50 nm on an ultraviolet photoresist [53]. Besides, the laser fluence, working distance, and irradiation time also

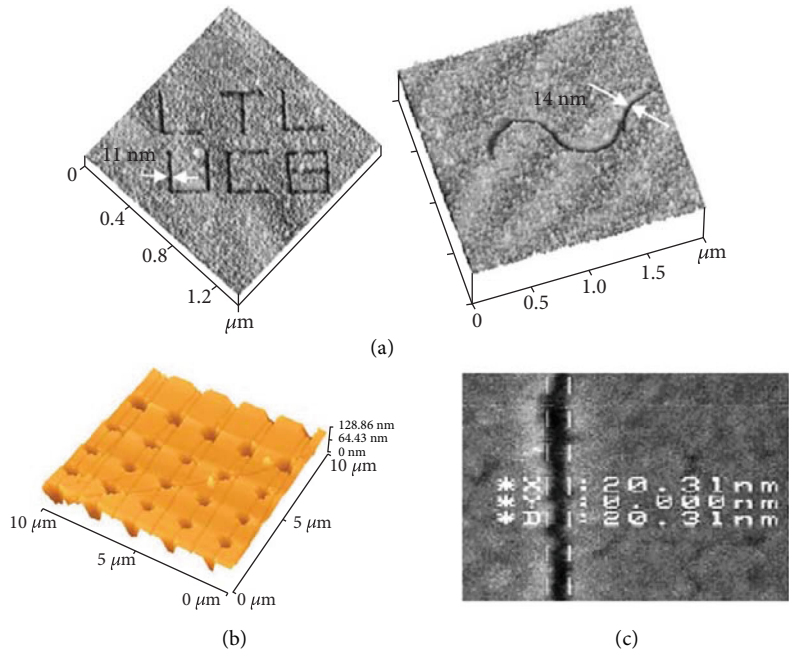

Figure 9: (a) AFM surface maps showing different symbols and curve patterns on gold film surface demonstrating the ability of complex shaping using femtosecond laser-assisted AFM processing, (b) AFM image of the dot arrays, and (c) AFM morphology of a nanoline structure fabricated by NSOM-assisted femtosecond laser nanolithography.

decide the fabricated feature sizes. The higher laser fluence and longer irradiation time will result in a larger feature size. With the fine controlling of the laser fluence and scanning speed, ~20 nm surface structuring can be realized. Compared with the traditional lithography, features with such high resolution by near-field femtosecond laser precision engineering can be used for the fabrication of nanoscale optoelectrical devices.

Microsphere array assisting laser processing is one of the wonderful techniques which can overcome the diffraction limit as well [136, 137]. Based on this method, micro-/nanostructure arrays can be created on the surface using a hexagonally close-packed monolayer of microspheres self-assembled on different substrates. The micro-/nanostructures perform various morphologies and distributions as laser fluence and microsphere size change, respectively [138]. The curved surface can also be processed since the microspheres can be assembled on flexible substrates. Mostly, the microsphere-assisted femtosecond laser irradiation is processed in contact mode, which means the microsphere should be directly deposited on the substrate. For instance, by using surface self-assembling a single layer of microspheres assisted 800 nm femtosecond laser irradiation, Zhou et al. created nanohole structures on the silica surface [139, 140]. Figure 10(a) presents the regular array of crater structures with a period of 6.84 μm, which consists of the diameter of the microsphere being used [140]. In the case of 35 J/cm^2 laser irradiation, the morphology of the nanohole structures characterized by AFM exhibits that the full-width at half-maximum of nanohole structures is 250 nm and the depth is about 150 nm, as shown in Figure 10(b). There is less debris on the irradiated area except for the microspheres in the center removed away and deposited in other locations. Since the photon energy of femtosecond laser (1.55 eV) is much smaller than the electronic bandgap of glass (5 eV), in this case, the MPA induced by the nonlinear effect significantly narrows the laser ablation area, which leads to the noncrack surface nanofabrication on the glass substrate. Thus, the microsphere-assisted femtosecond laser irradiation in contact mode is mostly used for periodic nanostructure creation.

In addition to the nanohole structures, the microsphere-assisted femtosecond laser fabrication can also realize arbitrary structures on sample surfaces under noncontact processing. As shown in Figure 10(c), Yan et al. combined the high index microsphere with a plano convex lens as a compound lens to create large area subwavelength surface manufacturing with programmed design [130]. The plano convex lens superlens can be assembled into a microscope, which leads to a subwavelength focus point at a micron-scale working distance. By using a side view observation system for real-time monitoring, and high spatial resolution nanoplatform for the fining control, the working distance between the microsphere and target can be well-tuned during the scanning pattern process. The single subwavelength creation of 230~ 350 nm feature size can be directly created. Combining with 355 nm UV laser irradiation, even ~100 nm nanostructures can be achieved. In summary, for the femtosecond laser processing in near field, the feature size achieved by such strategies is far lower than the incident laser wavelength, including NSOM- and AFM-assisted femtosecond laser fabrication. However, it requires the substrates have a smooth surface since the working distances of such strategies are mostly within a wavelength. As mentioned

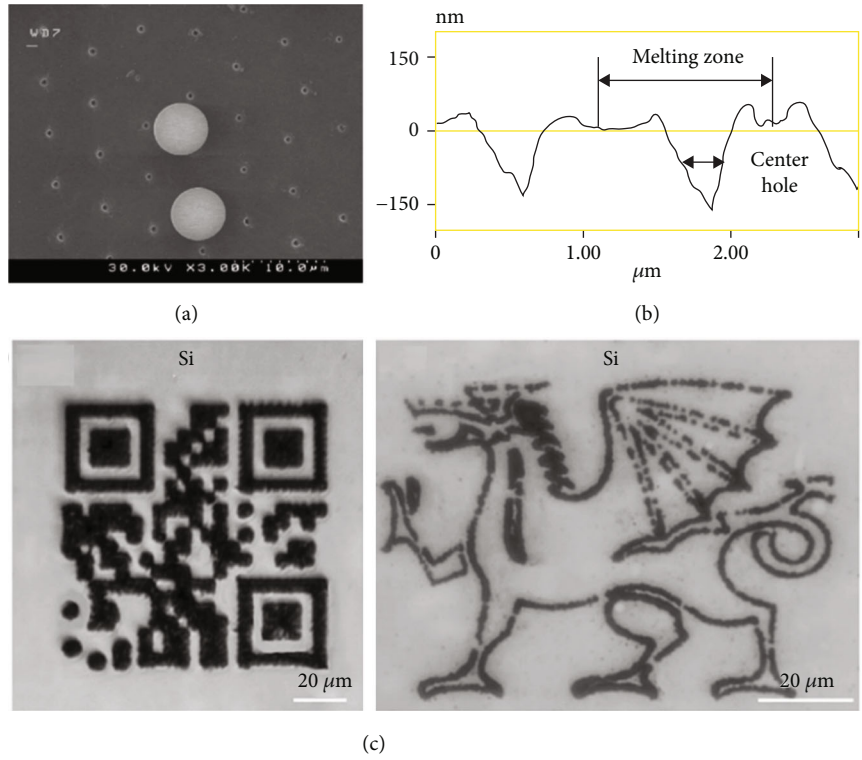

FIGURE 10: (a) SEM image of silica surface after single layer 6.84 μm silica microsphere-assisted femtosecond laser irradiation. (b) AFM cross-sectional image of the nano-hole structures created by using microsphere assisted femtosecond laser. (c) Arbitrary patterns including the QR code and Welsh dragon made on Si surfaces through removable microsphere assisted femtosecond laser irradiation.

above, the microsphere-assisted femtosecond laser operating on noncontact mode may be a feasible way to solve this issue. By lifting the microsphere up with a special holder, the working distance of this strategy can be increased to several micrometers. Furthermore, the microspheres can be fabricated in different shapes, which can modulate the optical energy distribution and reduce the focus size [141–143], even achieving the multifocal functionalities by patterning the Fresnel zone on the microsphere surface [144]. By using engineered microspheres under the noncontact mode, the microsphere-assisted femtosecond laser irradiation may be able to realize surface nanoscale precision engineering with large-area complex structures of arbitrary shapes.

5.2. Femtosecond Laser Nanostructuring in Far Field. The near-field femtosecond laser fabrication mostly requires a smooth target surface due to its short working distance. As a direct writing and mask-free technology, the femtosecond laser direct irradiation can create 3D microfluidics and complicated optofluidic devices in silica substrates and in far field. Using the femtosecond laser direct writing, Liao et al. created microfluidic channels with long lengths and designable 3D structures in porous silica with water immersing and the following postannealing process [145, 146]. As shown in Figures 11(a) and 11(b), nanochannels with spatial widths smaller than 50 nm inside the silica substrate were realized using femtosecond laser direct writing [131]. Such nanochannels are easy to expand to 3D microfluidic systems which can be simultaneously created inside the silica and used for the detection of single molecule DNA. Inspiring by the STED, Li et al. realized the creation of features with a minimum scalable resolution of 40 nm along the beam axis by processing spatial phase shaping of the laser beam deactivating [31]. With the fine controlling of laser fluence, the feature sizes of LIPSS can be well-tuned and the number of periodic nanostructures can be reduced to only a single nanogroove [132–135]. In this case, ~20 nm nanoline structures can be created inside the SiO_2 substrate. Combined with characteristics of femtosecond laser-induced multiphoton excitation and optical near-field effect, Li et al. found that the nanohole enhanced optical near field can provide very small resolution and reduce the required laser intensity for laser direct nanofabrication [33]. By tuning the polarization direction of the laser beam, it is feasible to create the nanogroove down to sub-50 nm with the designed pattern.

Recently, hybrid laser methods are widely used in the precision engineering of various materials. Especially, the strategy of double beams irradiation is feasible to achieve optical enhancement or nanofabrication [147–149]. As shown in Figure 11(c), our research group proposed a novel strategy that realizes the direct creation of 12 nm (λ/66) structures on semiconductor surfaces via the orthogonal polarized dual-femtosecond laser beam irradiation in far field and in ambient air [34]. The overlapping of the orthogonal polarized dual-femtosecond laser beams leads to the direction of nanoline structures almost parallel to the scanning direction,

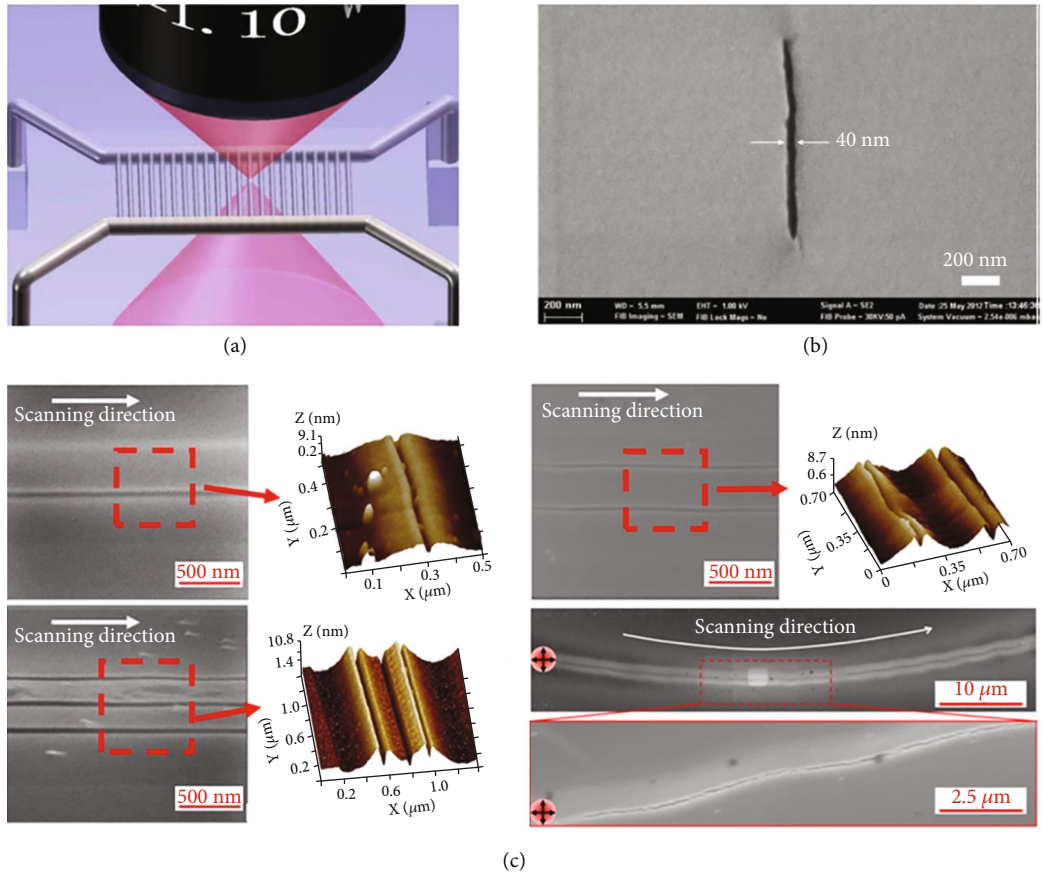

FIGURE 11: (a) Schematic diagram of the femtosecond laser direct fabricate 3D micro/nano-channels and (b) corresponding SEM cross-sectional image of a 40 nm nanochannel. (c) SEM and AFM images of the nanostructures fabricated using dual-femtosecond laser beams irradiation, including single-, double- and triple-line and the curve line structures.

regardless of the scanning path. Furthermore, multifemtosecond laser pulse irradiation-induced incubation effect under high repetition rate is considered the main reason for the ~12 nm creation. However, this method is still required to be further improved. In this strategy, the optical intensity distribution of on the focal plane is in a Gaussian distribution, which leads to a considerable melting region after femtosecond laser irradiation. Besides, some unnecessary ripples exist in the edge area. Thus, if the optical intensity distribution of the laser spot can be changed to flat-top distribution, the irradiated profile difference between the overlap region and non-overlap region will be more distinct, as well as the microbump due to the melting effect can be removed or decreased obviously. Thus, we suggest using dual flat-top beams to achieve ~10 nm nanostructures. In addition, the repetition rate plays an important role for the fabrication of dual-femtosecond laser beams induced nanostructures. By using a tunable repetition rate, the feature size, including the width and depth of such nanoline structures can be further controllable. Therefore, femtosecond precision engineering in nanoscale is an attractive method with great potentials. Although all the proposed near-field and far-field strategies still have limitations and need to be further improved, the nonlinear effect of the femtosecond laser is still a feasible way to realize sub-10 nm feature creation.

6. Challenges, Outlooks, and Conclusions

Up to now, the femtosecond laser has been widely developed and investigated in precision engineering with feature sizes from micron to nanoscale. However, there are still several challenges needed to be overcome. As shown in Figure 12, for the femtosecond laser precision engineering, three main challenges, including smaller HAZ, larger area/higher-speed processing, and feature size smaller than optical diffraction limit are demonstrated. The first main challenge in high-quality laser precision engineering to reduce the feature size from micron scale to nanoscale is how to achieve a small HAZ. To employ femtosecond laser-induced photothermal effect and photochemical reactions is a key issue required to be solved. Although the femtosecond laser is called as "cold process," there are still considerable thermal effects at high repetition rates and high laser fluences. Thus, it is significant to avoid and control the thermal effect properly during femtosecond laser fabrication. Meanwhile, the use of ultraviolet femtosecond laser can realize the modification of material's physical and chemical properties within dozens of femtoseconds, which can reduce the thermal effect and achieve smaller HAZ. Since it is hard to realize laser processing with high resolution and high efficiency simultaneously, the second key issue is to increase the efficiency to meet

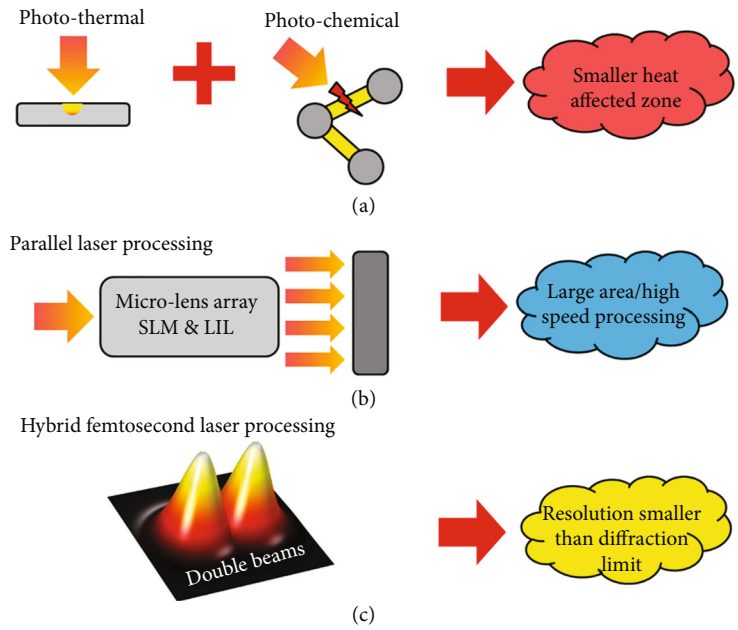

FIGURE 12: Schematic diagram of the challenges for femtosecond laser precision engineering: (a) smaller HAZ via photothermal and photochemical effects, (b) parallel laser processing for large area/high-speed processing, and (c) hybrid femtosecond laser processing to realize resolution smaller than the optical diffraction limit.

various industry demands. Parallel laser beam manufacturing is proposed as a versatile solution to fit both the requirements. As shown in Figure 12(b), MLA, spatial light modulator (SLM), and LIL are proposed as the most available strategies for high-efficiency femtosecond laser precision engineering. Especially, the MLA can provide over 10^5 nanostructure creation synchronously under single-pulse irradiation. Furthermore, combining with the phase change materials, the feature size fabricated by MLA-assisted femtosecond laser irradiation can be reduced to sub-100 nm. The last key challenge is how to realize nanomanufacturing of feature size smaller than the optical diffraction limit. The strategies using near-field optics, including NSOM, AFM, and microsphere, can create feature size in the order of ~10 nm. However, the weak signal of the evanescent wave due to the increase of working distance strongly constrains the actual application of near-field optics. For the NSOM and AFM, although the signal of evanescent wave can be increased via the surface plasmon enhancement effect, it is still hard to achieve high efficiency. Since the microsphere has been proved that can operate in noncontact mode [150, 151], it should be a promising near-field approach for the creation of sub-100 nm feature. Besides, the engineering microsphere also provides a feasible way to increase the working distance and modulate the optical focus property of microspheres. Furthermore, it is important to develop the femtosecond laser precision nanostructuring in far field and in ambient air since the near-field processing requires a short working distance, which limits the near-field nanofabrication to be only used on the samples with smooth surface and nonablation processing. For the femtosecond laser fabrication in far field, the obtained feature size is still confined by the optical diffraction limit. Thus, it should use some hybrid methods to achieve nanostructures for smaller feature sizes, as shown in Figure 12(c). By covering the substrate with water, the relative numerical aperture can be increased to 1.2. In this case, nanoline structures of 32 nm can be created on ZnO with 800 nm femtosecond laser irradiation due to the nonlinear threshold effect [132]. Furthermore, optical regulations such as STED and double-beam irradiation are both attractive and regarded as potential strategies to reduce the feature resolution to sub-10 nm. Especially, the double-beam irradiation, which can be extended to multiple beam irradiation, are also feasible to modulate the optical energy distribution in temporal and spatial domains simultaneously.

Despite the above three main challenges, the laser source and the optical processing systems are also key issues for high efficiency and quality femtosecond laser precision micro-/nanostructuring. To scale up the femtosecond laser micron processing, high-power laser sources with stable and good beam quality are significant. Besides, using of high repetition rate femtosecond laser oscillator for the nanostructuring should be a preferred choice in the future due to its low cost and high stability. The nanostage with higher scanning speed and motion resolution can improve the femtosecond laser micro-/nanoprocessing throughput as well. Furthermore, micro-/nanodevices fabricated by femtosecond laser tend to be more flexible, integrated, and intelligent. It requires that the femtosecond laser micro-/nanostructuring strategies can be suitable in different conditions. In summary, the ultrafast laser-matter interaction and its nonlinear effect make the femtosecond laser suitable for micron, submicron, and nanoscale precision engineering of various materials. First of all, the most attractive part of femtosecond micron-scale precision engineering is the capability of

processing semiconductors, hard brittle, and flexible materials. For a high laser fluence, the local absorption coefficient (<1 μm) of hard brittle material increases obviously, which leads to high efficiency and low surface roughness on the irradiated area. For the fabrication of flexible materials, the low HAZ of femtosecond laser irradiation is beneficial for the reduction of thermal deformation and the improvement of edge quality on the irradiated surface. Secondly, for the submicron processing, the femtosecond laser can be combined with other strategies, including MLA, LIL, and LIPSS, which are widely used for periodic surface patternings. Finally, the most fascinating of femtosecond laser precision engineering is the nanoscale feature creation. Although the near-field effect can obtain ~10 nm feature sizes, the short working distance and low efficiency make it hard to be employed for large area patterning. Noncontact microsphere-assisted femtosecond laser fabrication may be an available way to achieve large-area processing based on near-field effects. The sub-100 nm nanocreation working in far field and in atmosphere can solve the issues of short working distance and low output. Therefore, femtosecond laser irradiation is one of the most excellent and prospective processing methods for precision engineering. There are still many unexplained phenomena since the nonlinear interaction between the femtosecond laser and materials is complicated, which deserved to be further explored and investigated.

Conflicts of Interest

The authors declare that there is no conflict of interest regarding the publication of this article.

Acknowledgments

The authors are grateful for the support from Academic Research Fund Tier 2, Ministry of Education - Singapore (MOE2019-T2-2-147).

References

[1] P. van Assenbergh, E. Meinders, J. Geraedts, and D. Dodou, "Nanostructure and microstructure fabrication: from desired properties to suitable processes," *Small*, vol. 14, no. 20, pp. 1–24, 2018.

[2] E. Pomerantseva, F. Bonaccorso, X. Feng, Y. Cui, and Y. Gogotsi, "Energy storage: the future enabled by nanomaterials," *Science*, vol. 366, no. 6468, article eaan8285, 2019.

[3] X. G. Luo, D. P. Tsai, M. Gu, and M. Hong, "Extraordinary optical fields in nanostructures: from sub-diffraction-limited optics to sensing and energy conversion," *Chemical Society Reviews*, vol. 48, no. 8, pp. 2458–2494, 2019.

[4] H. G. Liu, W. Lin, and M. Hong, "Surface coloring by laser irradiation of solid substrates," *APL Photonics*, vol. 4, no. 5, pp. 1–13, 2019.

[5] D. J. Joe, S. Kim, J. H. Park et al., "Laser–material interactions for flexible applications," *Advanced Materials*, vol. 29, no. 26, p. 1606586, 2017.

[6] Y. D. Huang, J. Zhao, Z. Shu et al., "Ultrafast hole deformation revealed by molecular attosecond interferometry," *Ultrafast Science*, vol. 2021, article 9837107, 12 pages, 2021.

[7] Z. C. Ma, Y. L. Zhang, B. Han et al., "Femtosecond laser programmed artificial musculoskeletal systems," *Nature Communications*, vol. 11, no. 1, p. 4536, 2020.

[8] Y. Zhou, L. W. Chen, Z. R. du, Y. Cao, F. P. Li, and M. H. Hong, "Tunable optical nonlinearity of silicon nanoparticles in solid state organic matrix," *Optical Materials Express*, vol. 5, no. 7, p. 1606, 2015.

[9] Y. Song, C. Qu, M. Ma, and Q. Zheng, "Structural superlubricity based on crystalline materials," *Small*, vol. 16, no. 15, p. 1903018, 2020.

[10] Y. Zhang, D. J. Trainer, B. Narayanan et al., "One-dimensional lateral force anisotropy at the atomic scale in sliding single molecules on a surface," *Nano Letters*, vol. 21, no. 15, pp. 6391–6397, 2021.

[11] J. Li, T. Chen, T. Chen, and W. Lu, "Enhanced frictional performance in gradient nanostructures by strain delocalization," *International Journal of Mechanical Sciences*, vol. 201, article 106458, 2021.

[12] D. Berman, A. Erdemir, and A. V. Sumant, "Approaches for achieving superlubricity in two-dimensional materials," *ACS Nano*, vol. 12, no. 3, pp. 2122–2137, 2018.

[13] Z. Ma, X. Liu, X. Xu et al., "Bioinspired, highly adhesive, nanostructured polymeric coatings for superhydrophobic fire-extinguishing thermal insulation foam," *ACS Nano*, vol. 15, no. 7, pp. 11667–11680, 2021.

[14] Y. Zhao, Y. Su, X. Hou, and M. Hong, "Directional sliding of water: biomimetic snake scale surfaces," *Opto-Electronic Advances*, vol. 4, no. 4, pp. 210008–210013, 2021.

[15] L. Ji, X. Lv, Y. Wu, Z. Lin, and Y. Jiang, "Hydrophobic light-trapping structures fabricated on silicon surfaces by picosecond laser texturing and chemical etching," *Journal of Photonics for Energy*, vol. 5, no. 1, article 053094, 2015.

[16] B. Zhang, J. Jie, X. Zhang, X. Ou, and X. Zhang, "Large-scale fabrication of silicon nanowires for solar energy applications," *ACS Applied Materials & Interfaces*, vol. 9, no. 40, pp. 34527–34543, 2017.

[17] J. Yang, F. Luo, T. S. Kao et al., "Design and fabrication of broadband ultralow reflectivity black Si surfaces by laser micro/nanoprocessing," *Light: Science & Applications*, vol. 3, no. 7, article e185, 2014.

[18] F. Sima and K. Sugioka, "Ultrafast laser manufacturing of nanofluidic systems," *Nano*, vol. 10, no. 9, pp. 2389–2406, 2021.

[19] H. Wang, Y. L. Zhang, W. Wang, H. Ding, and H. B. Sun, "On-chip laser processing for the development of multifunctional microfluidic chips," *Laser & Photonics Reviews*, vol. 11, no. 2, p. 1600116, 2017.

[20] H. Wang, Y. L. Zhang, D. D. Han, W. Wang, and H. B. Sun, "Laser fabrication of modular superhydrophobic chips for reconfigurable assembly and self-propelled droplet manipulation," *PhotoniX*, vol. 2, no. 1, pp. 1–13, 2021.

[21] L. Yuan, S. Ding, and C. Wen, "Additive manufacturing technology for porous metal implant applications and triple minimal surface structures: a review," *Bioactive Materials*, vol. 4, no. 1, pp. 56–70, 2019.

[22] A. A. Lahcen, S. Rauf, T. Beduk et al., "Electrochemical sensors and biosensors using laser-derived graphene: a comprehensive review," *Biosensors & Bioelectronics*, vol. 168, article 112565, 2020.

[23] S. K. Saha, D. Wang, V. H. Nguyen, Y. Chang, J. S. Oakdale, and S. C. Chen, "Scalable submicrometer additive manufacturing," *Science*, vol. 366, no. 6461, pp. 105–109, 2019.

[24] T. C. Chong, M. H. Hong, and L. P. Shi, "Laser precision engineering: from microfabrication to nanoprocessing," *Laser & Photonics Reviews*, vol. 4, no. 1, pp. 123–143, 2010.

[25] J. del Barrio and C. Sánchez-Somolinos, "Light to shape the future: from photolithography to 4D printing," *Advanced Optical Materials*, vol. 7, no. 16, p. 1900598, 2019.

[26] K. Sugioka and Y. Cheng, "Femtosecond laser three-dimensional micro- and nanofabrication," *Applied Physics Reviews*, vol. 1, no. 4, pp. 1–35, 2014.

[27] A. Y. Vorobyev and C. Guo, "Direct femtosecond laser surface nano/microstructuring and its applications," *Laser & Photonics Reviews*, vol. 7, no. 3, pp. 385–407, 2013.

[28] Y. C. Jia, S. Wang, and F. Chen, "Femtosecond laser direct writing of flexibly configured waveguide geometries in optical crystals: fabrication and application," *Opto-Electronic Advances*, vol. 3, no. 10, article 190042, 2020.

[29] Y. Liao, Y. Shen, L. Qiao et al., "Femtosecond laser nanostructuring in porous glass with sub-50 nm feature sizes," *Optics Letters*, vol. 38, no. 2, pp. 187–189, 2013.

[30] R. Wollhofen, J. Katzmann, C. Hrelescu, J. Jacak, and T. A. Klar, "120 nm resolution and 55 nm structure size in STED-lithography," *Optics Express*, vol. 21, no. 9, pp. 10831–10840, 2013.

[31] N. Li, R. R. Gattass, E. Gershgoren, H. Hwang, and J. T. Fourkas, "Achieving $\lambda/20$ resolution by one-color initiation and deactivation of polymerization," *Science*, vol. 324, no. 5929, pp. 910–913, 2009.

[32] Y. Lin, M. H. Hong, W. J. Wang, Y. Z. Law, and T. C. Chong, "Sub-30 nm lithography with near-field scanning optical microscope combined with femtosecond laser," *Applied Physics A: Materials Science & Processing*, vol. 80, no. 3, pp. 461–465, 2005.

[33] Z. Z. Li, L. Wang, H. Fan et al., "O-FIB: far-field-induced near-field breakdown for direct nanowriting in an atmospheric environment," *Light: Science & Applications*, vol. 9, no. 1, pp. 1–7, 2020.

[34] Z. Y. Lin, H. G. Liu, L. F. Ji, W. Lin, and M. Hong, "Realization of ~10 nm features on semiconductor surfaces via femtosecond laser direct patterning in far field and in ambient air," *Nano Letters*, vol. 20, no. 7, pp. 4947–4952, 2020.

[35] T. H. Maiman, "Stimulated optical radiation in ruby," *Nature*, vol. 187, no. 4736, pp. 493-494, 1960.

[36] N. Bloembergen, "Laser-material interactions; fundamentals and applications," *AIP Conference Proceedings*, vol. 288, no. 3, pp. 3–8, 1993.

[37] G. X. Chen, M. H. Hong, T. S. Ong et al., "Carbon nanoparticles based nonlinear optical liquid," *Carbon*, vol. 42, no. 12–13, pp. 2735–2737, 2004.

[38] B. N. Chichkov, C. Momma, S. Nolte, F. Alvensleben, and A. Tünnermann, "Femtosecond, picosecond and nanosecond laser ablation of solids," *Applied Physics*, vol. 63, no. 2, pp. 109–115, 1996.

[39] S. Kawata, H. B. Sun, T. Tanaka, and K. Takada, "Finer features for functional microdevices," *Nature*, vol. 412, no. 6848, pp. 697-698, 2001.

[40] Z. C. Ma, Y. L. Zhang, B. Han, Q. D. Chen, and H. B. Sun, "Femtosecond-laser direct writing of metallic micro/nanostructures: from fabrication strategies to future applications," *Small Methods*, vol. 2, no. 7, pp. 1–20, 2018.

[41] P. Kiefer, V. Hahn, M. Nardi et al., "Sensitive photoresists for rapid multiphoton 3d laser micro- and nanoprinting," *Advanced Optical Materials*, vol. 8, no. 19, p. 2000895, 2020.

[42] W. Kaiser and C. G. B. Garrett, "Two-photon excitation in CaF_2: Eu^{2+}," *Physical Review Letters*, vol. 7, no. 6, pp. 229–231, 1961.

[43] R. R. Gattass, L. R. Cerami, and E. Mazur, "Micromachining of bulk glass with bursts of femtosecond laser pulses at variable repetition rates," *Optics Express*, vol. 14, no. 12, pp. 5279–5284, 2006.

[44] D. Gómez and I. Goenaga, "On the incubation effect on two thermoplastics when irradiated with ultrashort laser pulses: broadening effects when machining microchannels," *Applied Surface Science*, vol. 253, no. 4, pp. 2230–2236, 2006.

[45] C. Gaudiuso, H. Kämmer, F. Dreisow, A. Ancona, A. Tünnermann, and S. Nolte, "Ablation of silicon with bursts of femtosecond laser pulses," in *Frontiers in Ultrafast Optics: Biomedical, Scientific, and Industrial Applications XVI*, vol. 9740no. 3, p. 974017, San Francisco, California, USA, March 2016.

[46] C. Y. Shih, M. V. Shugaev, C. Wu, and L. V. Zhigilei, "Generation of subsurface voids, incubation effect, and formation of nanoparticles in short pulse laser interactions with bulk metal targets in liquid: molecular dynamics study," *Journal of Physical Chemistry C*, vol. 121, no. 30, pp. 16549–16567, 2017.

[47] F. di Niso, C. Gaudiuso, T. Sibillano, F. P. Mezzapesa, A. Ancona, and P. M. Lugarà, "Role of heat accumulation on the incubation effect in multi-shot laser ablation of stainless steel at high repetition rates," *Optics Express*, vol. 22, no. 10, pp. 12200–12210, 2014.

[48] H. G. Liu, W. X. Lin, Z. Y. Lin, L. Ji, and M. Hong, "Self-organized periodic microholes array formation on aluminum surface via femtosecond laser ablation induced incubation effect," *Advanced Functional Materials*, vol. 29, no. 42, p. 1903576, 2019.

[49] V. Nathan, S. S. Mitra, and A. H. Guenther, "Review of multiphoton absorption in crystalline solids," *Journal of the Optical Society of America B: Optical Physics*, vol. 2, no. 2, p. 294, 1985.

[50] A. Ródenas, M. Gu, G. Corrielli et al., "Three-dimensional femtosecond laser nanolithography of crystals," *Nature Photonics*, vol. 13, no. 2, pp. 105–109, 2019.

[51] E. Abbe, "Beiträge zur theorie des mikroskops und der mikroskopischen wahrnehmung," *Archiv für Mikroskopische Anatomie und Entwicklungsmechanik*, vol. 9, no. 1, pp. 413–468, 1873.

[52] D. van Labeke, D. Barchiesi, and F. Baida, "Optical characterization of nanosources used in scanning near-field optical microscopy," *Journal of the Optical Society of America. A*, vol. 12, no. 4, p. 695, 1995.

[53] Y. Lin, M. H. Hong, W. J. Wang et al., "Surface nanostructuring by femtosecond laser irradiation through near-field scanning optical microscopy," *Sensors and Actuators A*, vol. 133, no. 2, pp. 311–316, 2007.

[54] M. Hong, Z. Chen, M. Tang, L. Shi, and T. C. Chong, "Femtosecond laser irradiation for functional micro-/nanostructure fabrication," in *2009 Conference on Lasers & Electro Optics & The Pacific Rim Conference on Lasers and Electro-Optics*, pp. 3-4, Shanghai, China, August 2009.

[55] D. Ghezzi, R. M. Vazquez, R. Osellame et al., "Femtosecond laser microfabrication of an integrated device for optical release and sensing of bioactive compounds," *Sensors*, vol. 8, no. 10, pp. 6595–6604, 2008.

[56] L. Kelemen, E. Lepera, B. Horváth, P. Ormos, R. Osellame, and R. Martínez Vázquez, "Direct writing of optical microresonators in a lab-on-a-chip for label-free biosensing," *Lab on a Chip*, vol. 19, no. 11, pp. 1985–1990, 2019.

[57] Z. Hou, Y. Sun, Q. Li, X. Fan, and R. Cheng, "Smart bio-gel optofluidic Mach–Zehnder interferometers multiphoton-lithographically customized with chemo-mechanical-opto transduction and bio-triggered degradation," *Lab on a Chip*, vol. 20, no. 20, pp. 3815–3823, 2020.

[58] S. Shaikh, D. Singh, M. Subramanian et al., "Femtosecond laser induced surface modification for prevention of bacterial adhesion on 45S5 bioactive glass," *Journal of Non-Crystalline Solids*, vol. 482, pp. 63–72, 2017.

[59] A. Daskalova, L. Angelova, A. Carvalho et al., "Effect of surface modification by femtosecond laser on zirconia based ceramics for screening of cell-surface interaction," *Applied Surface Science*, vol. 513, no. 9, article 145914, 2020.

[60] Z. Wang, Z. du, J. K. Y. Chan, S. H. Teoh, E. S. Thian, and M. Hong, "Direct laser microperforation of bioresponsive surface-patterned films with through-hole arrays for vascular tissue-engineering application," *ACS Biomaterials Science & Engineering*, vol. 1, no. 12, pp. 1239–1249, 2015.

[61] J. N. Wang, Y. Q. Liu, Y. L. Zhang et al., "Wearable superhydrophobic elastomer skin with switchable wettability," *Advanced Functional Materials*, vol. 28, no. 23, pp. 1–8, 2018.

[62] A. Royon, Y. Petit, G. Papon, M. Richardson, and L. Canioni, "Femtosecond laser induced photochemistry in materials tailored with photosensitive agents [invited]," *Optical Materials Express*, vol. 1, no. 5, p. 866, 2011.

[63] A. Bellucci, M. Mastellone, M. Girolami et al., "Nanocrystalline lanthanum boride thin films by femtosecond pulsed laser deposition as efficient emitters in hybrid thermionic-photovoltaic energy converters," *Applied Surface Science*, vol. 513, no. 2, article 145829, 2020.

[64] M. H. Chen, Y. H. Tseng, Y. P. Chao et al., "Effects on organic photovoltaics using femtosecond-laser-treated indium tin oxides," *ACS Applied Materials & Interfaces*, vol. 8, no. 38, pp. 24989–24993, 2016.

[65] D. Differt, B. Soleymanzadeh, F. Lükermann, C. Strüber, W. Pfeiffer, and H. Stiebig, "Enhanced light absorption in nanotextured amorphous thin-film silicon caused by femtosecond-laser materials processing," *Solar Energy Materials & Solar Cells*, vol. 135, pp. 72–77, 2015.

[66] C. H. Crouch, J. E. Carey, J. M. Warrender, M. J. Aziz, E. Mazur, and F. Y. Génin, "Comparison of structure and properties of femtosecond and nanosecond laser-structured silicon," *Applied Physics Letters*, vol. 84, no. 11, pp. 1850–1852, 2004.

[67] R. Torres, V. Vervisch, M. Halbwax et al., "Femtosecond laser texturization for improvement of photovoltaic cells: black silicon," *Journal of Optoelectronics and Advanced Materials*, vol. 12, no. 3, pp. 621–625, 2010.

[68] R. Buividas, S. Rekštytė, M. Malinauskas, and S. Juodkazis, "Nano-groove and 3D fabrication by controlled avalanche using femtosecond laser pulses," *Optical Materials Express*, vol. 3, no. 10, p. 1674, 2013.

[69] M. Malinauskas, A. Žukauskas, G. Bičkauskaitė, R. Gadonas, and S. Juodkazis, "Mechanisms of three-dimensional structuring of photo-polymers by tightly focussed femtosecond laser pulses," *Optics Express*, vol. 18, no. 10, pp. 10209–10221, 2010.

[70] K. T. Paula, G. Gaál, G. F. B. Almeida et al., "Femtosecond laser micromachining of polylactic acid/graphene composites for designing interdigitated microelectrodes for sensor applications," *Optics and Laser Technology*, vol. 101, pp. 74–79, 2018.

[71] R. Zhang, C. Huang, J. Wang, H. Zhu, P. Yao, and S. Feng, "Micromachining of 4H-SiC using femtosecond laser," *Ceramics International*, vol. 44, no. 15, pp. 17775–17783, 2018.

[72] C. Wu, X. Fang, F. Liu, X. Guo, R. Maeda, and Z. Jiang, "High speed and low roughness micromachining of silicon carbide by plasma etching aided femtosecond laser processing," *Ceramics International*, vol. 46, no. 11, pp. 17896–17902, 2020.

[73] B. Ali, I. V. Litvinyuk, and M. Rybachuk, "Femtosecond laser micromachining of diamond: current research status, applications and challenges," *Carbon*, vol. 179, pp. 209–226, 2021.

[74] X. Q. Liu, B. F. Bai, Q. D. Chen, and H. B. Sun, "Etching-assisted femtosecond laser modification of hard materials," *Opto-Electronic Advances*, vol. 2, no. 9, pp. 19002101–19002114, 2019.

[75] Y. Hanada, K. Sugioka, I. Miyamoto, and K. Midorikawa, "Double-pulse irradiation by laser-induced plasma-assisted ablation (LIPAA) and mechanisms study," *Applied Surface Science*, vol. 248, no. 1–4, pp. 276–280, 2005.

[76] M. H. Hong, K. Sugioka, D. J. Wu et al., "Laser-induced plasma-assisted ablation and its applications," in *Third International Symposium on Laser Precision Microfabrication*, vol. 4830no. 2, p. 408, Osaka, Japan, February 2003.

[77] J. Zhang, K. Sugioka, and K. Midorikawa, "Laser-induced plasma-assisted ablation of fused quartz using the fourth harmonic of a Nd^+: YAG laser," *Applied Physics A: Materials Science & Processing*, vol. 67, no. 5, pp. 545–549, 1998.

[78] H. G. Liu, W. Lin, and M. Hong, "Hybrid laser precision engineering of transparent hard materials: challenges, solutions and applications," *Light: Science & Applications*, vol. 10, no. 1, p. 162, 2021.

[79] M. H. Hong, K. Sugioka, Y. F. Lu, K. Midorikawa, and T. C. Chong, "Laser microfabrication of transparent hard materials and signal diagnostics," *Applied Surface Science*, vol. 186, no. 1–4, pp. 556–561, 2002.

[80] T. U. Rahman, Z. U. Rehman, S. Ullah et al., "Laser-induced plasma-assisted ablation (LIPAA) of glass: effects of the laser fluence on plasma parameters and crater morphology," *Optics and Laser Technology*, vol. 120, no. 3, article 105768, 2019.

[81] U. Sarma and S. N. Joshi, "Machining of micro-channels on polycarbonate by using laser-induced plasma assisted ablation (LIPAA)," *Optics and Laser Technology*, vol. 128, no. 4, article 106257, 2020.

[82] H. Liu, Y. Li, W. Lin, and M. Hong, "High-aspect-ratio crack-free microstructures fabrication on sapphire by femtosecond laser ablation," *Optics and Laser Technology*, vol. 132, no. 6, article 106472, 2020.

[83] L. Xu, H. Liu, H. Zhou, and M. Hong, "One-step fabrication of metal nanoparticles on polymer film by femtosecond

LIPAA method for SERS detection," *Talanta*, vol. 228, article 122204, 2021.

[84] C. Pan, K. Chen, B. Liu et al., "Fabrication of micro-texture channel on glass by laser-induced plasma-assisted ablation and chemical corrosion for microfluidic devices," *Journal of Materials Processing Technology*, vol. 240, pp. 314–323, 2017.

[85] S. Xu, B. Liu, C. Pan et al., "Ultrafast fabrication of microchannels and graphite patterns on glass by nanosecond laser-induced plasma-assisted ablation (LIPAA) for electro-fluidic devices," *Journal of Materials Processing Technology*, vol. 247, no. 4, pp. 204–213, 2017.

[86] Y. Li, H. Liu, and M. Hong, "High-quality sapphire microprocessing by dual-beam laser induced plasma assisted ablation," *Optics Express*, vol. 28, no. 5, pp. 6242–6250, 2020.

[87] H. L. Liu, M. H. Hong, F. Chen, and P. Wu, "Visible waveguide lasers based on femtosecond laser inscribed cladding waveguides in Pr:YLF crystal," in *2018 Conf. Lasers Electro-Optics, CLEO: Science and Innovations 2018*, pp. 9-10, San Jose, California USA, May 2018.

[88] H. L. Liu, J. R. Vazquez de Aldana, M. H. Hong, and F. Chen, "Femtosecond laser inscribed Y-branch waveguide in Nd: YAG crystal: fabrication and continuous-wave lasing," *IEEE Journal of Selected Topics in Quantum Electronics*, vol. 22, no. 2, pp. 227–230, 2016.

[89] H. Liu, S. Luo, B. Xu et al., "Femtosecond-laser micromachined Pr:YLF depressed cladding waveguide: Raman, fluorescence, and laser performance," *Optical Materials Express*, vol. 7, no. 11, p. 3990, 2017.

[90] L. Li, Z. Li, W. Nie, C. Romero, J. R. V. de Aldana, and F. Chen, "Femtosecond-laser-written s-curved waveguide in Nd:YAP crystal: fabrication and multi-gigahertz lasing," *Journal of Lightwave Technology*, vol. 38, no. 24, pp. 6845–6852, 2020.

[91] D. Ganin, K. Lapshin, A. Obidin, and S. Vartapetov, "Single-pulse perforation of thin transparent dielectrics by femtosecond lasers," *Applied Physics A: Materials Science & Processing*, vol. 123, no. 5, pp. 1–7, 2017.

[92] Y. Berg, Z. Kotler, and Y. Shacham-Diamand, "Holes generation in glass using large spot femtosecond laser pulses," *Journal of Micromechanics and Microengineering*, vol. 28, no. 3, article 035009, 2018.

[93] F. Baset, K. Popov, A. Villafranca et al., "Femtosecond laser induced surface swelling in poly-methyl methacrylate," *Optics Express*, vol. 21, no. 10, pp. 12527–12538, 2013.

[94] F. Zhang, X. Dong, K. Yin et al., "Temperature effects on the geometry during the formation of micro-holes fabricated by femtosecond laser in PMMA," *Optics and Laser Technology*, vol. 100, pp. 256–260, 2018.

[95] Z. Wang, S. H. Teoh, M. Hong et al., "Dual-microstructured porous, anisotropic film for biomimicking of endothelial basement membrane," *ACS Applied Materials & Interfaces*, vol. 7, no. 24, pp. 13445–13456, 2015.

[96] D. Zheren, C. Lianwei, W. Dacheng et al., "3D micro-concrete hybrid structures fabricated by femtosecond laser two-photon polymerization for biomedical and photonic applications," in *2016 IEEE International Conference on Industrial Technology (ICIT)*, vol. 5, pp. 1108–1114, Taipei, China, March 2016.

[97] Y. L. Zhang, Y. Tian, H. Wang et al., "Dual-3D femtosecond laser nanofabrication enables dynamic actuation," *ACS Nano*, vol. 13, no. 4, pp. 4041–4048, 2019.

[98] A. Michalek, S. Qi, A. Batal et al., "Sub-micron structuring/texturing of diamond-like carbon-coated replication masters with a femtosecond laser," *Applied Physics A: Materials Science & Processing*, vol. 126, no. 2, pp. 1–12, 2020.

[99] T. Karkantonis, A. Gaddam, T. L. See, S. S. Joshi, and S. Dimov, "Femtosecond laser-induced sub-micron and multi-scale topographies for durable lubricant impregnated surfaces for food packaging applications," *Surface and Coatings Technology*, vol. 399, no. 6, article 126166, 2020.

[100] P. Umenne and V. V. Srinivasu, "Femtosecond-laser fabrication of micron and sub-micron sized S-shaped constrictions on high T c superconducting YBa2Cu3O7−x thin films: ablation and lithography issues," *Journal of Materials Science: Materials in Electronics*, vol. 28, no. 8, pp. 5817–5826, 2017.

[101] Y. Li and M. Hong, "Parallel laser micro/nano-processing for functional device fabrication," *Laser & Photonics Reviews*, vol. 14, no. 3, p. 1900062, 2020.

[102] Y. Lin, M. H. Hong, T. C. Chong et al., "Ultrafast-laser-induced parallel phase-change nanolithography," *Applied Physics Letters*, vol. 89, no. 4, article 041108, 2006.

[103] C. S. Lim, M. H. Hong, Y. Lin et al., "Sub-micron surface patterning by laser irradiation through microlens arrays," *Journal of Materials Processing Technology*, vol. 192-193, pp. 328–333, 2007.

[104] Z. C. Chen, N. R. Han, Z. Y. Pan, Y. D. Gong, T. C. Chong, and M. H. Hong, "Tunable resonance enhancement of multi-layer terahertz metamaterials fabricated by parallel laser micro-lens array lithography on flexible substrates," *Optical Materials Express*, vol. 1, no. 2, p. 151, 2011.

[105] A. Borowiec and H. K. Haugen, "Subwavelength ripple formation on the surfaces of compound semiconductors irradiated with femtosecond laser pulses," *Applied Physics Letters*, vol. 82, no. 25, pp. 4462–4464, 2003.

[106] J. Bonse, S. Hohm, S. V. Kirner, A. Rosenfeld, and J. Kruger, "Laser-induced periodic surface structures-a scientific evergreen," *IEEE Journal of Selected Topics in Quantum Electronics*, vol. 23, no. 3, pp. 109–123, 2017.

[107] J. E. Sipe, J. F. Young, J. S. Preston, and H. M. van Driel, "Laser-induced periodic surface structure. I. Theory," *Physical Review B*, vol. 27, no. 2, pp. 1141–1154, 1983.

[108] M. Huang, F. Zhao, Y. Cheng, N. Xu, and Z. Xu, "Origin of laser-induced near-subwavelength ripples: interference between surface plasmons and incident laser," *ACS Nano*, vol. 3, no. 12, pp. 4062–4070, 2009.

[109] J. Bonse, A. Rosenfeld, and J. Krüger, "On the role of surface plasmon polaritons in the formation of laser-induced periodic surface structures upon irradiation of silicon by femtosecond-laser pulses," *Journal of Applied Physics*, vol. 106, no. 10, article 104910, 2009.

[110] Y. C. Guan, W. Zhou, Z. L. Li, H. Y. Zheng, G. C. Lim, and M. H. Hong, "Femtosecond laser-induced ripple structures on magnesium," *Applied Physics A: Materials Science & Processing*, vol. 115, no. 1, pp. 13–18, 2014.

[111] C. Hnatovsky, V. G. Shvedov, and W. Krolikowski, "The role of light-induced nanostructures in femtosecond laser micromachining with vector and scalar pulses," *Optics Express*, vol. 21, no. 10, pp. 12651–12656, 2013.

[112] N. Livakas, E. Skoulas, and E. Stratakis, "Omnidirectional iridescence via cylindrically- polarized femtosecond laser processing," *Opto-Electronic Advances*, vol. 3, no. 5, pp. 190035–190039, 2020.

[113] S. A. Jalil, J. Yang, M. ElKabbash, C. Cong, and C. Guo, "Formation of controllable 1D and 2D periodic surface structures on cobalt by femtosecond double pulse laser irradiation," *Applied Physics Letters*, vol. 115, no. 3, article 031601, 2019.

[114] F. Fraggelakis, G. Mincuzzi, J. Lopez, I. Manek-Hönninger, and R. Kling, "Controlling 2D laser nano structuring over large area with double femtosecond pulses," *Applied Surface Science*, vol. 470, no. 11, pp. 677–686, 2019.

[115] W. Liu, L. Jiang, W. Han et al., "Manipulation of LIPSS orientation on silicon surfaces using orthogonally polarized femtosecond laser double-pulse trains," *Optics Express*, vol. 27, no. 7, pp. 9782–9793, 2019.

[116] H. J. Gerritsen and M. E. Heller, "Thermally engraved gratings using a giant-pulse laser," *Journal of Applied Physics*, vol. 38, no. 5, pp. 2054–2057, 1967.

[117] P. Simon and J. Ihlemann, "Machining of submicron structures on metals and semiconductors by ultrashort UV-laser pulses," *Applied Physics A: Materials Science & Processing*, vol. 63, no. 5, pp. 505–508, 1996.

[118] B. Li, L. Jiang, X. Li et al., "Flexible gray-scale surface patterning through spatiotemporal-interference-based femtosecond laser shaping," *Adv. Opt. Mater.*, vol. 6, no. 24, pp. 1801021–1801027, 2018.

[119] J. P. Spallas, R. D. Boyd, J. A. Britten et al., "Fabrication of sub-0.5 μm diameter cobalt dots on silicon substrates and photoresist pedestals on 50 cm×50 cm glass substrates using laser interference lithograph," *Journal of Vacuum Science & Technology B: Microelectronics and Nanometer Structures*, vol. 14, no. 3, pp. 2005–2007, 1996.

[120] M. H. Hong, C. H. Liu, F. Ma et al., "Large-area plasmonic structures fabricated by laser nanopatterning and their applications," in *Laser-based Micro- and Nanopackaging and Assembly III*, vol. 7202no. 2, p. 72020K, San Jose, California, USA, February 2009.

[121] M. N. Liu, L. Wang, Y. H. Yu, and A. W. Li, "Biomimetic construction of hierarchical structures via laser processing," *Optical Materials Express*, vol. 7, no. 7, p. 2208, 2017.

[122] L. Dong, Z. Zhang, R. Ding et al., "Controllable superhydrophobic surfaces with tunable adhesion fabricated by laser interference lithography," *Surface and Coatings Technology*, vol. 372, no. 5, pp. 434–441, 2019.

[123] E. Stankevičius, E. Daugnoraitė, and G. Račiukaitis, "Mechanism of pillars formation using four-beam interference lithography," *Optics and Lasers in Engineering*, vol. 116, pp. 41–46, 2019.

[124] J. Xu, Z. Wang, Z. Zhang, D. Wang, and Z. Weng, "Fabrication of moth-eye structures on silicon by direct six-beam laser interference lithography," *Journal of Applied Physics*, vol. 115, no. 20, article 203101, 2014.

[125] A. Wang, L. Jiang, X. Li et al., "Nanoscale material redistribution induced by spatially modulated femtosecond laser pulses for flexible high-efficiency surface patterning," *Optics Express*, vol. 25, no. 25, pp. 31431–31442, 2017.

[126] Y. Nakata, M. Yoshida, K. Osawa, and N. Miyanaga, "Fabricating a regular hexagonal lattice structure by interference pattern of six femtosecond laser beams," *Applied Surface Science*, vol. 417, pp. 69–72, 2017.

[127] A. Chimmalgi, T. Y. Choi, C. P. Grigoropoulos, and K. Komvopoulos, "Femtosecond laser aperturless near-field nanomachining of metals assisted by scanning probe microscopy," *Applied Physics Letters*, vol. 82, no. 8, pp. 1146–1148, 2003.

[128] I. Falcón Casas and W. Kautek, "Subwavelength nanostructuring of gold films by apertureless scanning probe lithography assisted by a femtosecond fiber laser oscillator," *Nanomaterials*, vol. 8, no. 7, p. 536, 2018.

[129] W. J. Wang, R. Zhao, L. P. Shi et al., "Nonvolatile phase change memory nanocell fabrication by femtosecond laser writing assisted with near-field optical microscopy," *Journal of Applied Physics*, vol. 98, no. 12, article 124313, 2005.

[130] B. Yan, L. Yue, J. Norman Monks et al., "Superlensing plano-convex-microsphere (PCM) lens for direct laser nanomarking and beyond," *Optics Letters*, vol. 45, no. 5, pp. 1168–1171, 2020.

[131] Y. Liao, Y. Cheng, C. Liu et al., "Direct laser writing of sub-50 nm nanofluidic channels buried in glass for three-dimensional micro-nanofluidic integration," *Lab on a Chip*, vol. 13, no. 8, pp. 1626–1631, 2013.

[132] J. Liu, T. Jia, K. Zhou et al., "Direct writing of 150 nm gratings and squares on ZnO crystal in water by using 800 nm femtosecond laser," *Optics Express*, vol. 22, no. 26, pp. 32361–32370, 2014.

[133] X. He, A. Datta, W. Nam, L. M. Traverso, and X. Xu, "Sub-diffraction limited writing based on laser induced periodic surface structures (LIPSS)," *Scientific Reports*, vol. 6, no. 1, pp. 1–8, 2016.

[134] V. R. Bhardwaj, E. Simova, P. P. Rajeev et al., "Optically produced arrays of planar nanostructures inside fused silica," *Physical Review Letters*, vol. 96, no. 5, pp. 1–4, 2006.

[135] R. Taylor, C. Hnatovsky, and E. Simova, "Applications of femtosecond laser induced self-organized planar nanocracks inside fused silica glass," *Laser & Photonics Reviews*, vol. 2, no. 1–2, pp. 26–46, 2008.

[136] Z. L. Wu, Y. N. Qi, X. J. Yin et al., "Polymer-based device fabrication and applications using direct laser writing technology," *Polymers*, vol. 11, no. 3, p. 553, 2019.

[137] J. H. Soh, M. Wu, G. Gu, L. Chen, and M. Hong, "Temperature-controlled photonic nanojet via $_{VO\_2}$ coating," *Applied Optics*, vol. 55, no. 14, pp. 3751–3756, 2016.

[138] Y. Zhou, M. H. Hong, J. Y. H. Fuh et al., "Direct femtosecond laser nanopatterning of glass substrate by particle-assisted near-field enhancement," *Applied Physics Letters*, vol. 88, no. 2, pp. 023110–023113, 2006.

[139] Y. Zhou, M. H. Hong, J. Y. H. Fuh et al., "Nanopatterning mask fabrication by femtosecond laser irradiation," *Journal of Materials Processing Technology*, vol. 192-193, pp. 212–217, 2007.

[140] Y. Zhou, M. H. Hong, J. Y. H. Fuh, L. Lu, B. S. Lukyanchuk, and Z. B. Wang, "Near-field enhanced femtosecond laser nano-drilling of glass substrate," *Journal of Alloys and Compounds*, vol. 449, no. 1–2, pp. 246–249, 2008.

[141] M. Wu, R. Chen, J. Soh et al., "Super-focusing of center-covered engineered microsphere," *Scientific Reports*, vol. 6, no. 1, pp. 1–7, 2016.

[142] M. X. Wu, B. J. Huang, R. Chen et al., "Modulation of photonic nanojets generated by microspheres decorated with concentric rings," *Optics Express*, vol. 23, no. 15, pp. 20096–20103, 2015.

[143] Y. Zhou and M. Hong, "Formation of a three-dimensional bottle beam via an engineered microsphere," *Photonics Res.*, vol. 9, no. 8, pp. 11121–11130, 2021.

[144] Y. Zhou, R. Ji, J. Teng, and M. Hong, "Wavelength-tunable focusing via a Fresnel zone microsphere," *Optics Letters*, vol. 45, no. 4, pp. 852–855, 2020.

[145] Y. Liao, Y. Ju, L. Zhang et al., "Three-dimensional microfluidic channel with arbitrary length and configuration fabricated inside glass by femtosecond laser direct writing," *Optics Letters*, vol. 35, no. 19, pp. 3225–3227, 2010.

[146] Y. Liao, J. Song, E. Li et al., "Rapid prototyping of three-dimensional microfluidic mixers in glass by femtosecond laser direct writing," *Lab on a Chip*, vol. 12, no. 4, pp. 746–749, 2012.

[147] L. Qin, Y. Huang, F. Xia et al., "5 nm nanogap electrodes and arrays by super-resolution laser lithography," *Nano Letters*, vol. 20, no. 7, pp. 4916–4923, 2020.

[148] Z. Lin, L. Ji, and M. Hong, "Enhancement of femtosecond laser-induced surface ablation via temporal overlapping double-pulse irradiation," *Photonics Res.*, vol. 8, no. 3, p. 271, 2020.

[149] R. Zhou, S. Lin, Y. Ding, H. Yang, K. Ong Yong Keng, and M. Hong, "Enhancement of laser ablation via interacting spatial double-pulse effect," *Opto-Electronic Advances*, vol. 1, no. 8, pp. 18001401–18001406, 2018.

[150] L. W. Chen, Y. Zhou, Y. Li, and M. Hong, "Microsphere enhanced optical imaging and patterning: from physics to applications," *Applied Physics Reviews*, vol. 6, no. 2, article 021304, 2019.

[151] G. X. Wu and M. Hong, "Optical nano-imaging via microsphere compound lenses working in non-contact mode," *Optics Express*, vol. 29, no. 15, pp. 23073–23082, 2021.